PROBLEMS IN MOTION OF COMPRESSIBLE FLUIDS AND REACTION PROPULSION

Thesis

by

Hsue-shen Tsien

In Partial Fulfillment of the Requirements for the Degree of Doctor of Philosophy

California Institute of Technology

Pasadena, California

1938

ACKNOWLEDGEMENTS

The author wants first to express his deep gratitude to Dr. Theodore von Karman. Not only the subjects for PART (I), (II) and (III) were suggested by Dr. von Karman but his constant guiding and help were also essential for carrying out these studies. His inspiration and his warm personality have won the author's highest respect and love.

The author also wants to thank Dr. Harry Bateman for his help in summing the series in PART (IV) and general discussions. During the preparation of PART (IV) the author was very much benefited by frequent discussions with Mr. Frank J. Malina who was also very kind in helping the author in numerical computations and figures in PART (IV).

TABLE OF CONTENTS

PART (I)

BOUNDARY LAYER IN COMPRESSIBLE FLUIDS

The solution of flow problems in which the density is variable is in general very difficult; hence, every case in which an exact or even an approximate solution of the equations of the motion of compressible fluids can be obtained has considerable theoretical interest. Several authors noticed that the theory of the laminar boundary layer can be extended to the case of compressible fluids moving with arbitrarily high velocities without encountering insurmountable mathematical difficulties. Busemann (Ref. 1) established the equations and calculated the velocity profile for one speed ratio. (By speed ratio is understood the ratio of the airspeed to the velocity of sound.) Frankl (Ref. 2) also made an analysis of the same problem, however, it is complicated and depends on several arbitrary approximations. Von Karman (Ref. 3) obtained a first approximation by a simple but apparently not sufficiently exact calculation. Hence, in Section (I), a better method for the solution of the problem is developed.

The boundary layer theory for very high velocities is not without practical interest. First, the statement can be found often in technical and semi-technical literature on rockets and similar high-speed devices that the skin friction becomes more and more significant at high speeds. Of course,

it is known that with increasing Reynolds Number, the skin friction coefficient is decreasing, i.e., the skin friction becomes relatively small in comparison with the drag produced by wave formation or direct shock. Since high-speed flight will be performed mostly at high altitude where the air is of very low density, so that the kinematic viscosity is large, the resulting Reynolds Number will be relatively small in spite of the high speed.

Another interesting point in the theory of the boundary layer in compressible fluids is the thermodynamic aspect of the problem. In the case of low speeds the influence of the heat produced in the boundary layer can be neglected both in the calculation of the drag and of the heat transferred to the wall. In the case of high speeds, however, the heat produced in the boundary layer is not negligible, but determines the direction of heat flow. In Section (II) a few simple examples of heat flow through the boundary layer are discussed.

It has been found necessary in most parts of this analysis to make the assumption of laminar flow. This assumption was found necessary because of the lamentable state of knowledge concerning the laws of turbulent flow of compressible fluids at high speeds. This assumption is somewhat justified by the fact that - as mentioned above - in many problems where

the results of this paper can be applied, the Reynolds Number is relatively small, so that a considerable portion of the boundary layer is probably, de facto, laminar. Ackeret (Ref.4) called attention to the possibility that the stability conditions in supersonic flow might be quite different from those occuring in flow with low velocities.

Recently Küchemann (Ref.5) studied the stability of a linear profile near a wall under small sinuous disturbance, and shown that as the velocity ratio increases, the flow is unstable at increasing wave length of disturbance. However, he assumed that the gas is non-viscous and the sound velocity is constant. Both assumptions tend to limit the usefulness of the theory, especially the later one. Because the constancy of velocity of gas implies the constancy of gas temperature, which unfortunately is far from the truth for a perfect gas as will be shown in later calculations of this section. In spite of these uncertainties, some calculations of this section, as will be pointed out, are also applicable to turbulent flow. In other cases, as in the calculation of drag, the assumption of laminar flow surely gives at least the lower limit of its value.

Section (I)

If the x -axis is taken along the plate in the direction of the free stream, the y -axis perpendicular to the

plate, and u and v indicate the x and y components of the velocity at any point, then the simplified equation of motion in the boundary layer is, i.e. stationary flow

$$\rho u \frac{\partial u}{\partial x} + \rho v \frac{\partial u}{\partial y} = \frac{\partial}{\partial y}\left(\mu \frac{\partial u}{\partial y}\right) \tag{1.1}$$

where both the density ρ and the viscosity μ are variables.

The equation of continuity in this case is

$$\frac{\partial}{\partial x}(\rho u) + \frac{\partial}{\partial y}(\rho v) = 0 \; . \tag{1.2}$$

A third equation determines the energy balance between the heat produced by viscous dissipation and the heat transferred by conduction and convection. With the same simplification as used in Eqs.(1.1 and (1.2), one can write

$$\rho u \frac{\partial}{\partial x}(c_p \cdot T) + \rho v \frac{\partial}{\partial y}(c_p \cdot T) = \frac{\partial}{\partial y}\left(\lambda \frac{\partial T}{\partial y}\right) + \mu \left(\frac{\partial u}{\partial y}\right)^2 \tag{1.3}$$

where c_p is the specific heat at constant pressure, and λ is the coefficient of heat conduction. If Prandtl's number, $c_p \mu / \lambda$ is assumed to be equal to 1, then it can be easily shown that both Eqs. (1.1) and (1.3) can be satisfied by equating the temperature T to a certain parabolic function of the velocity u only. Indeed, introducing $c_p T = f(u)$

into equation (1.3) and replacing λ by $c_p \mu$, one obtains

$$\left(\rho u \frac{\partial u}{\partial x} + \rho v \frac{\partial u}{\partial y}\right) f'(u) = \frac{\partial}{\partial y}\left(\mu \cdot \frac{\partial u}{\partial y}\right) f'(u) + \mu\left[f''(u) + 1\right]\left(\frac{\partial u}{\partial y}\right)^2$$

Hence Eq. (1.3) is reduced to Eq. (1.1) if $f''(u) = -1$

or

$$c_p T = C_1 + C_2 u - \frac{u^2}{2}$$

where C_1, C_2 are constants. Denoting the wall temperature $(u = 0)$ by T_w and remembering that $T = T_0$ for $u = U$ where U = free stream velocity, C_1, C_2 can be expressed in terms of T_w, T_0 and

$$\frac{T}{T_0} = \frac{T_w}{T_0} - \left(\frac{T_w}{T_0} - 1\right)\frac{u}{U} + \frac{\gamma-1}{2} M^2 \frac{u}{U}\left(1 - \frac{u}{U}\right) \tag{1.4}$$

Differentiating Eq. (1.4) one obtains

$$\frac{1}{T_0}\left(\frac{\partial T}{\partial y}\right)_w = \frac{1}{U}\left[\frac{\gamma-1}{2}M^2-\left(\frac{T_w}{T_0}-1\right)\right]\left(\frac{\partial u}{\partial y}\right)_w \qquad (1.5)$$

where the subscript w refers to conditions existing at the surface of the plate. Now $(\partial u/\partial y)_w$ is always positive; therefore, if $[(\gamma-1)/2]M^2 > (T_w/T_0) - 1$

heat is transferred from the fluid to the wall; if

$$[(\gamma-1)/2]M^2 = T_w/T_0 - 1$$

there is no heat transfer between the fluid and the wall; and if

$$[(\gamma-1)/2]M^2 < T_w/T_0 - 1$$

heat is transferred from the wall to the fluid. If there is no heat transfer, the energy content per unit mass $(u^2/2) + c_p T$ is constant in the whole region of the boundary layer. (Ref.6)

The pressure being constant the relation between ρ and T is,

$$\rho = \rho_0 \frac{T_0}{T} \qquad (1.6)$$

The expression for the viscosity based on the kinetic theory of gases is

$$\mu = \mu_0 \left(\frac{T}{T_0}\right)^{\frac{1}{2}} \tag{1.7}$$

However, the following formula is in closer agreement with experimental data

$$\mu = \mu_0 \left(\frac{T}{T_0}\right)^{0.76} \tag{1.7a}$$

Busemann (Ref. 1) calculated the limiting case for which $[(\gamma-1)/2]M^2 = (T_{ws}/T_0) - 1$ using Eq. (1.7) and found that for a high Mach's number, the velocity profile is approximately linear. Von Karman (Ref. 3), using the linear velocity profile, the integral relation between the friction and the momentum, and Eq. (1.7) found that

$$C_f = \frac{\text{Frictional drag per unit width of plate}}{(\rho_0 U^2/2) \quad x \quad \text{length of plate}}$$

$$= \Theta\sqrt{\frac{\mu_0}{\rho_0 U x}} \left\{1 + \frac{\gamma-1}{2} M^2\right\}^{-\frac{1}{4}} \tag{1.8}$$

The dimensions quantity Θ shown in Table (1.1) is a function of Mach's number only.

However, if Eq. (1.7a) is used, then

$$C_f = \Theta \sqrt{\frac{\mu_0}{\rho_0 U x}} \left\{ 1 + \frac{\gamma - 1}{2} M^2 \right\}^{-0.12} \tag{1.8a}$$

Table 1.1

M	0	1	2	5	10	∞
Θ	1.16	1.20	1.25	1.39	1.50	1.57

It is evident that this linear approxmiation is not satisfactory for small values of Mach's number. For $M = 0$, the case is the same as the Blasius solution (Ref. 7) for incompressible fluids for which Θ is 1.328.

To solve the problem more rigorously, one has to resort to Eqs. (1.1) and (1.2). By introducing the stream function ψ which is defined by

$$\frac{\rho}{\rho_0} u = \frac{\partial \psi}{\partial y}, \qquad -\frac{\rho}{\rho_0} v = \frac{\partial \psi}{\partial x}$$

the equation of continuity, Eq. (1.2), is satisfied automatically. Now if in Eq. (1.1) ψ is introduced as the independent variable as was done by von Mises (Ref. 8) in his simplification of the boundary layer equation for incompressible fluids then

$$\frac{\partial}{\partial y} = \frac{\rho u}{\rho_0} \frac{\partial}{\partial \psi}, \qquad \frac{\partial}{\partial x} = \frac{\partial}{\partial n} - \frac{\rho}{\rho_0} v \frac{\partial}{\partial \psi}$$

where n is a coordinate measured in normal direction to

ψ coordinate. Using these new coordinates, the following relations exist

$$\rho u \frac{\partial u}{\partial x} + \rho v \frac{\partial u}{\partial y} = \rho u \frac{\partial u}{\partial x}$$

and

$$\mu \frac{\partial u}{\partial y} = \mu \frac{\rho u}{\rho_0} \frac{\partial u}{\partial \psi}$$

therefor Eq. (1.1) can be written as

$$\frac{\partial u}{\partial x} = \frac{\partial}{\partial \psi}\left[\mu \frac{\rho}{\rho_0} u \frac{\partial u}{\partial \psi}\right] \tag{1.9a}$$

Eq. (1.9a) can be put into non-dimensional form by introducing the following set of new quantities:

$$\begin{aligned} u^* &= u/U \\ x^* &= x/L \\ \psi^* &= (\psi/UL)\sqrt{\rho_0 UL/\mu_0} = (\psi/UL)\sqrt{R} \\ \rho^* &= \rho/\rho_0 \\ \mu^* &= \mu/\mu_0 \end{aligned} \tag{1.9b}$$

where L is a convenient length, say length of the plate, and R is the corresponding Reynold's Number, then Eq. (1.9a) becomes

$$\frac{\partial u^*}{\partial x^*} = \frac{\partial}{\partial \psi^*}\left(u^* \rho^* \mu^* \frac{\partial u^*}{\partial \psi^*}\right) \tag{1.9}$$

Eq. (1.9) can be further simplified by introducing a new dependent variable $\zeta = \psi^*/\sqrt{n^*}$, then

$$-\frac{\zeta}{2}\frac{du^*}{d\zeta} = \frac{d}{d\zeta}\left(u^*\rho^*\mu^*\frac{du^*}{d\zeta}\right) \qquad (1.10)$$

This can be solved by the method of successive approximations. As ρ^* and μ^* are functions of temperature only as shown in Eqs. (1.6 and (1.7) or (1.7a) and the temperature is a function of u^* then by starting with the known Blasius' solution (Ref. 7) the right-hand side of Eq. (1.10) can be expressed in terms of ζ . Therefore, one can write $u^*\rho^*\mu^* = f(\zeta)$ and Eq. (1.10) becomes $-\frac{\zeta}{2}\frac{du^*}{d\zeta} = \frac{d}{d\zeta}\left[f(\zeta)\frac{du^*}{d\zeta}\right]$

Consequently, the solution of Eq. (1.10) is

$$u^* = C\int_0^\zeta \frac{F}{f}\,d\zeta \qquad \text{where} \qquad F = e^{-\int_0^\zeta \frac{\zeta\,d\zeta}{f}}$$

(1.11)

and C is determined by the boundary condition that at $\zeta = \infty$

$$u^* = 1, \qquad \frac{1}{C} = \int_0^\infty \frac{F}{f}\,d\zeta \qquad (1.11a)$$

In the actual computation, two methods of evaluating the integrals in Eqs. (1.11) and (1.11a) are used. For small values of ζ , $\zeta < 0.2$, the function u^* and $f(\zeta)$ are expanded in a power series of ζ . Due to the uniform convergence of the power series for sufficiently

small values of ζ , the integration is carried out term by term. For values of $\zeta > 0.2$, numerical integration is used.

A second approximation can be made based upon the value of u^* obtained from Eq. (1.11). It has been found in the cases investigated that the third and fourth approximation gives sufficient accuracy, if the velocity profile of next smaller Mach's number is used as the starting point of calculating the velocity profile of next larger Mach's number.

Having computed the final u^* , the y corresponding to u^* can be calculated in the following way:

It is known from Eq. (1.9b) that

$$\zeta = \frac{\psi^*}{\sqrt{n^*}} = \frac{\sqrt{R}\,\frac{\psi}{UL}}{\sqrt{n^*}}$$

Then remembering the definition of ψ , one has

$$\frac{\partial \zeta}{\partial y^*} = \frac{\sqrt{R}}{\sqrt{n^*}}\,\rho^* u^*$$

However due to the small slope of stream lines,

$$\frac{\partial \zeta}{\partial y^*} \approx \frac{d\zeta}{dy^*}$$

Hence

$$dy^* = \frac{\sqrt{n^*}}{\sqrt{R}} \frac{d\zeta}{\rho^* u^*} \tag{1.12a}$$

or

$$\frac{\sqrt{R}}{\sqrt{n^*}} y^* = \frac{y}{\sqrt{\frac{x \mu_0}{U \rho_0}}} = \int_0^{\zeta} \frac{d\zeta}{\rho^* u^*} \tag{1.12}$$

Here the expansion of $\rho^* u^*$ in a power series for small values of ζ is especially useful due to the singularity of integrand at $\zeta = 0$.

The skin friction can be computed by using momentum law, i.e.,

$$\text{Drag} = D = \left\{ \int_0^{\infty} \rho u (U - u) dy \right\}_{x=L}$$

Using Eq. (1.12a), on has

$$dy = L\, dy^* = \frac{\sqrt{n^*}\, L\, d\zeta}{\sqrt{R}\, \rho^* u^*}$$

thus

$$D = \left\{ L \rho_0 U^2 \frac{\sqrt{n^*}}{\sqrt{R}} \right\}_{x=L} \int_0^{\infty} (1 - u^*) d\zeta$$

But $n^* = \frac{n}{L} \approx \frac{x}{L}$, therefore

$$\{n^*\}_{x=L} = 1$$

Hence

$$D = \frac{L \rho_0 U^2}{\sqrt{R}} \int_0^\infty (1 - u^*) d\zeta$$

Thus the skin friction coefficient can be computed as

$$C_f = \frac{D}{\frac{\rho_0}{2} U^2 L} = \frac{2 \int_0^\infty (1 - u^*) d\zeta}{\sqrt{R}} \qquad (1.13)$$

The velocity profile, the temperature distribution, and the frictional drag coefficient are calculated for different values of the Mach's number of the free stream, for the case

$$[(\gamma - 1)/2] M^2 = (T_w/T_0) - 1$$

using the approximate viscosity relation of Eq. (1.7a). The results are shown in Figs. 1.2 and 1.3. The velocity profiles for high speeds are very nearly linear, but it can be seen that the wall temperature for greater Mach's numbers is very high. If the free stream temperature is 40°F., then the wall temperature will be 1600°F., 3620°F., 6540°F., and 10,170°F. for

Mach's numbers of 4, 6, 8, and 10, respectively. Therefore, there is no doubt that the law of viscosity as expressed by Eq. (1.7a) will not hold. Also at such high temperatures, the heat transfer due to radiation cannot be neglected. The effect of radiation will be the equalization of gas temperature. In the extreme case of complete equalization, the temperature will be constant throughout the layer and due to the assumed constant pressure throughout the field, the density and viscosity of gas will be also constant throuhgout the field. Then the velocity profile will be again that calculated by Blasius for incompressible fluid. By this reasoning, the actual velocity profile for large Mach's number when radiation cannot be neglected is something between the Blasius profile and that shown in Fig. 3.

The change in the constant $C_f \sqrt{R}$ is appreciable, but not great. It decreases from 1.328 for $M = 0$ to 0.975 for $M = 10$, or about 30 percent. However, for $0 < M < 3$ the change of the constant is very small.

Fig. 1.2 also shows that Eq. (1.8a) which was obtained by using the linear approximation is fairly accurate for very high Mach's numbers.

As examples, consider first a projectile and second, a wingless sounding rocket. Taking the diameter of

the projectile to be 6 in., the length 24 in., the velocity 1500 ft./sec. and the altitude 32,800 ft. (10 km.), then the Reynold's Number based on the total length is 7.86×10^6 and the speed ratio is 1.52. From Fig 1.2 the skin friction coefficient is

$$C_f = (1.286 \times 10^{-3}) / \sqrt{7.86} = 0.000459$$

Changing the skin friction coefficient (based on the skin area) to the drag coefficient (based on the maximum cross-section), one obtains

$$C_{D_f} = 0.0055$$

The drag coefficient due to wave formation taken from Kent's experiments (Ref. 9) is $C_{D_W} - 0.190$

Therefore the ratio of skin friction to wave resistance is $0.0055/0.190 = 0.029$.

However, the ratio is greatly changed in the case of the rocket. Taking the diameter of the rocket to be 9 in., the length 8 ft., and the altitude of flight 50 km. (see Appendix) (164,000 ft.), the velocity 3400 ft./sec., then the Reynold's Number based on a density ratio at that altitude of 0.00067 and temperature 25°C. (deduced from data on meteors) is 6.14×10^5, and the speed ratio is 3.00. From Fig. 1.2, the skin friction coefficient is

$$C_f = (1.213 \times 10^{-2}) / \sqrt{11.4} = 0.00360$$

Then

$$C_{D_f} = 0.123$$

The drag coefficient due to wave formation from Kent's experiment (Ref. 9) is

$$C_{D_W} = 0.100$$

Therefore, the ratio of skin friction and wave resistance is now 0.123/0.100 = 1.23. If the boundary layer is partly turbulent, the ratio will be even greater. This shows clearly the importance of skin friction in the case of a slender body moving with high speed in extremely rarified air. It also disproves the belief that wave resistance would always be the predominating part in the total drag of a body moving with a velocity higher than that of sound. The reason underlying this fact can be easily understood when one recalls that the wave resistance of a body is approximately directly proportional to the velocity, while the skin friction is proportional to the velocity raised to a power between 1.5 and 2. Therefore, the ratio of skin friction to wave resistance increases with the speed. With very high velocities and high kinematic viscosity, the wave resistance may even be a negligible portion of the total drag of the body.

Section (II)

In order to point out the thermodynamic aspect of the problem two cases will be considered: the flow of a hot fluid along a surface which is kept at a constant temperature inferior to that of the fluid, and the case of a hot wall

cooled by a fluid of lower temperature. The problems treated in this part have been discussed before in two very interesting papers by L. Crocco (Ref. 6). He especially gives an elegant treatment of the cooling problem in the case of very high velocities ("Hyperaviation"). The author feels that his treatment is somewhat more general and extended than Crocco's previous analysis.

An interesting general relation between the heat transferred through the wall and the frictional drag can be obtained using the assumption that Prandtl's number, i.e., the ratio $c_p \mu / \lambda$, is equal to unity. The same assumption was used also in the previous calculations. It is remarkable that the relation holds also as well for laminar as for turbulent flow. The heat flow q per unit time and unit area of the wall surface is

$$q = \lambda_w (\partial T / \partial y)_w$$

and the frictional drag τ per unit area is

$$\tau = \mu_w (\partial u / \partial y)_w$$

Using Eq. (1.4) the ratio q/τ can be calculated from the relation

$$\frac{q}{\tau} = \frac{\lambda_w}{\mu_w} \frac{T_0}{U} \left[\left(1 - \frac{T_w}{T_0} \right) + \frac{\gamma - 1}{2} M^2 \right] \qquad (1.14)$$

where T_0 is the absolute temperature, and U the velocity of the fluid in the free stream, T_w the absolute

temperature at the wall, λ_w and μ_w are the heat conduction and viscosity coefficients of the fluid corresponding to the wall temperature and M denotes Mach's number. Substituting $M = 0$ one obtains from Eq. (1.14)

$$\frac{q}{\tau} = \frac{\lambda_w}{\mu_w} \frac{T_0 - T_w}{U} = \frac{c_p (T_0 - T_w)}{U} \tag{1.15}$$

This is the relation known as Prandtl's or G. I. Taylor's formula, first discovered by O. Reynolds. Hence Eq. (1.14) gives the correction of this result for compressibility effects.

In the case $T_0 > T_w$ i.e., when the wall is colder than the free stream, the effect of compressibility is to increase the heat transferred through the wall. However, it would be erroneous to interpret this result as an "improvement" in cooling because at high speed the heat produced in the boundary layer is of the same order as the heat transferred through the wall. In order to determine the efficiency of the cooling a complete heat balance must be made. For this purpose Eq. (1.14) does not give sufficient information and the velocity and the temperature distribution in the boundary layer must be computed. Such calculations were carried out for the particular assumption $T_w = T_0/4$ i.e., for the particular case in which the absolute temperature of the wall is kept constant

at a value equal to one-fourth of the temperature of the hot fluid. With the same assumption for the variation of μ as in Section (I), the results shown in Fig. 1.2 and Fig. 1.4 were obtained. The variation of $C_f\sqrt{R}$ with M is similar to that obtained in the case without heat conduction through the wall. Also the highest temperature in the boundary layer is very high for extreme Mach numbers. However, the temperature maximum occurs some distance from the wall.

The heat transferred from the boundary layer to the wall can be calculated as follows:

By means of Eq. (1.12a), one has

$$\frac{\partial u}{\partial y} = \frac{U}{L}\frac{\partial u^*}{\partial y^*} = \frac{U}{L}\frac{du^*}{d\zeta}\frac{d\zeta}{dy^*}$$

$$= \frac{U\sqrt{R}}{L\sqrt{x^*}}(\rho^* u^*)\frac{du^*}{d\zeta}$$

Hence

$$C_f = \frac{D}{\frac{\rho_0}{2}U^2L} = \frac{1}{\frac{\rho_0}{2}U^2L}\int_0^L \mu_w\left(\frac{\partial u}{\partial y}\right)_{y=0} dx$$

$$= \frac{1}{\frac{\rho_0}{2}U^2L}\frac{U\sqrt{R}\mu_0}{\sqrt{L}}\frac{\rho_w}{\rho_0}\frac{\mu_w}{\mu_0}\left\{u^*\frac{du^*}{d\zeta}\right\}_w\int_0^L\frac{dx}{\sqrt{x}}$$

$$= \frac{4}{\sqrt{R}}\frac{\rho_w}{\rho_0}\frac{\mu_w}{\mu_0}\left\{u^*\frac{du^*}{d\zeta}\right\}_w$$

Therefore, combining the above two equations,

$$\left(\frac{\partial u}{\partial y}\right)_w = \frac{U}{L}\frac{\sqrt{R}}{\sqrt{n^*}}\left(\frac{\mu_0}{\mu_w}\right)\frac{\sqrt{R}\, C_f}{4} \tag{1.16}$$

Using Eq. (1.7a) and substituting Eq. (1.16) into Eq. (1.5), then

$$\left(\frac{\partial T}{\partial y}\right)_w = K_1 \frac{T_0\sqrt{R}}{2L\sqrt{n^*}} \tag{1.17}$$

where $K_1 = (4^{0.76}/2)(0.75 + \frac{\gamma-1}{2}M^2)\sqrt{R}\, C_f$, as given in Table 1.2. Therefore, the heat transferred to a strip of unit width of the wall of length L per unit time is equal to

$$Q_1 = \int_0^L \left(\lambda \frac{\partial T}{\partial y}\right)_w dx \cong \frac{K_1 \lambda_w T_0 \sqrt{R}}{2\sqrt{L}} \int_0^L \frac{dx}{\sqrt{x}}$$

$$= K_1 \lambda_w T_0 \sqrt{R}$$

Now the increase in heat content of the gas per unit time by flowing from $x = 0$ to $x = L$ can be calculated as

$$Q_2 = \int_0^\infty \left\{ \rho u c_p (T_0 - T) dy \right\}_{x=L} - \rho_0 U c_p T_0 \sqrt{\frac{\mu_0 L}{U \rho_0}} \int_0^\infty (1 - T^*) d\zeta$$

$$= \lambda_0 T_0 \sqrt{R} \int_0^\infty (1 - T^*) d\zeta = \lambda_w \left(\frac{\lambda_0}{\lambda_w}\right) T_0 \sqrt{R} \int_0^\infty (1 - T^*) d\zeta$$

$$= \lambda_w \left(\frac{\mu_0}{\mu_w}\right) T_0 \sqrt{R} \int_0^\infty (1 - T^*) d\zeta = K_2 \lambda_w T_0 \sqrt{R} \tag{1.19}$$

The viscous dissipation of gas in the boundary layer of unit width plate per unit time is thus

$$Q = Q_1 + Q_2 \tag{1.20}$$

Table 1.2

M	K_1
0	1.53
1	1.93
2	3.12
5	10.53
10	33.98

The total heat balance at different Mach's numbers is shown in Fig. 1.5. The "dissipation" curve represents in dimensionless form the heat produced by friction per unit time and unit width of the plate. The lower curve shows the increase (or decrease) of the heat content per unit time and unit width. The difference of the ordinates corresponds to the heat transferred through the wall. It is seen that cooling takes place for $M < 2.6$. Beyond this limit more heat is produced by friction than the amount which can be transferred to the wall and, as a matter of fact, the fluid is heated.

In the case $T_w > T_0$ i.e., when the wall is hotter than the free stream, the ratio between the heat transfer and the drag decreases with increasing Mach's number. This is shown in Fig. 1.6 where the ordinate represents the ratio between q/τ with compressibility effect (according to Eq. (1.14)) to q/τ without compressibility effect (according) to Eq. (1.15)). The calculation was carried out for a gas temperature of -55° F. and a wall temperature of 180° F. and 300°F. It is seen that there is no cooling in the former case for $M > 1.69$ and in the latter case for $M > 2.08$. However, the decrease of cooling efficiency is appreciable even at much lower speeds. This emphasizes the benefit of the reduction of the speed of cooling air and the relatively poor efficiency of cooling surfaces exposed directly

to a high-speed airstream. The curves in Fig. 1.6 being derived from Eq. (1.14) apply to laminar as well as to turbulent motion.

APPENDIX TO PART (I)

ON THE VALIDITY OF THEORY IN VERY RAREFIED AIR

The hydrodynamic equation holds so long as the mean free path of the molecules is small in comparison with the thickness of the boundary layer. For this case the thickness of the boundary layer is zero at the nose, however, at a distance $\frac{1}{4}$ of the length of the rocket it already amounts to 3.2 cm., while the calculated mean free path of the air molecules at the altitude considered is about 1.1×10^{-2} cm. Hence it appears that even for this case the theory can be safely applied. This conclusion is substantiated by the experimental results of H. Ebert in "Darstellung der Strömungsvorgange von Gasen bei neidrigen Drucken mittels Reynoldsscher Zahlen", Zeitschrift für Physik, Bd. 85, S. 561-564, 1933.

REFERENCES ON PART (I)

1. Busemann, A., Gas-strömung mit laminaren Grenzschicht entlang einer Platte, Z.A.M.M., Vol. 15, S. 23, 1935.

2. Frankl, Laminar Boundary Layer of Compressible Fluids, Trans. of the Joukowsky Central Aero-Hydrodynamical Institute, Moscow, 1934, (Russian).

3. Karman, Th. von, The Problem of Resistance in Compressible Fluids, V. Convengo della Foundazione Alessandro Volta (Tema: Le Alte Velocita in Aviazione), Reale Accademia D'Italia, Rome.

4. Ackeret, J., Über Luftkraft bei sehr grossen Geschwindigkeiten insbesondere bei ebenen Strömungen, Helvetica Physica Acta, Vol. 1, S. 301-322, (1928).

5. Küchemann, D., Störungsbewegungen in einer Gasströmung mit Grenzschicht, Z.A.M.M., Vol. 18, S. 207-222, (1938).

6. Crocco, L., Su di un valore massimo del coefficient di transmissione del calore da una lamina piana a un fluido scorrente, Rendiconti R. Accademia dei Lincei, Vol. 14, fasc. 490-496, 1931.
   Crocco, L., Sulla Transmissione del calore da una lamina piana un fluido scorrente ad alta velocita, L'Aerotecnica, Vol. 12, fasc. 181-197, 1932.

7. Blasius, H., Grenzschichten in Flüssigkeiten mit kleiner Reibung, Zeit. F. Math. u. Phys., Bd. 56, S. 1, 1908.

8. von Mises, Bemerkung zur Hydrodynamik, Z.A.M.M., Vol. 7, S. 425, 1927.

9. Kent, R. H., The Rôle of Model Experiment in Projectile Design, Mechanical Engineering. Vol. 54, pages 641-646, 1932.

PART (II)

SUPERSONIC FLOW OVER AN INCLINED BODY OF REVOLUTION

The aerodynamic forces acting on a projectile can be divided into three parts: the resistance or drag in the direction of the axis of the body, the lift in the direction perpendicular to the axis of the body, and the forces due to the rotation of the body (Magnus effect). The first component, the resistance, is, of course, the most important one, because it is the predominating factor in determining the range of the projectile. However, in the case of an actual projectile, inclination and rotation are always present, and therefore, accurate calculation of range is impossible without considering the second and third components of aerodynamic forces, i.e., the lift and the forces due to rotation of the body. It is found that the solution of von Karman and Moore (Ref. 1) for the linearized hydrodynamical equation of axial flow over a slender body of revolution can easily be generalized to the cases in which the projectile is inclined to the flight path. Strictly speaking, the solution is applicable only to a very slender body inclined at a small angle to the flight path, because second order quantities of the disturbance due to the presence of the body are neglected. However, for the case of

axial flow over a cone, von Karman-Moore's first approximation (Ref. 1) differs very little from the exact solution of Taylor and Maccoll (Ref. 2) for vortex angles up to 40°. Therefore, it is expected that the first approximation of the lift force as obtained in this paper can be applied to a pointed projectile with fair accuracy.

If ϕ is the potential of the small disturbance velocity due to the presence of a body of revolution whose axis coincides with the x-axis, then the linearized equation of motion of compressible fluids in cylindrical co-ordinates x, r, and θ is

$$\left(1-\frac{V^2}{c^2}\right)\frac{\partial^2\phi}{\partial x^2}+\frac{1}{r}\frac{\partial\phi}{\partial r}+\frac{\partial^2\phi}{\partial r^2}+\frac{1}{r^2}\frac{\partial^2\phi}{\partial\theta^2}=0 \qquad (1.1)$$

In this equation, V is the velocity of the undisturbed flow for which the velocity of sound is c. If the direction of the undisturbed flow coincides with the axis of the body, then ϕ is independent of θ, and Eq. (1.1) reduced to

$$\left(1-\frac{V^2}{c^2}\right)\frac{\partial^2\phi}{\partial x^2}+\frac{1}{r}\frac{\partial\phi}{\partial r}+\frac{\partial^2\phi}{\partial r^2}=0 \qquad (1.2)$$

The solution of this equation when the velocity of the undisturbed flow is greater than the velocity of

sound, is the same as that for a two-dimensional wave diverging from a center. It was obtained by Levi-Civita (Ref. 3) and by H. Lamb (Ref. 4). Von Karman and Moore (Ref. 1) applied it to the present case and showed that it can be expressed as a source distribution given by the potential

$$\phi_1 = \int_{\cosh^{-1}\frac{x}{\alpha r}}^{0} f_1(x - \alpha r \cosh u)\, du \qquad (1.3)$$

where $\alpha = \sqrt{(V/c)^2 - 1}$. Analogy with a similar case of flow of an incompressible fluid leads one to expect the solution of Eq. (1.1) to be a doublet distribution given by the potential

$$\phi_2 = -\alpha \cos\theta \int_{\cosh^{-1}\frac{x}{\alpha r}}^{0} f(x - \alpha r \cosh u) \cosh u \, du \qquad (1.4)$$

This can be shown to be true, because, if the solution of Eq. (1.1) is of the form

$$\phi_2 = \cos\theta \; F(x, r)$$

then Eq. (1.1) reduces to

$$\left(1 - \frac{V^2}{c^2}\right)\frac{\partial^2 F}{\partial x^2} + \frac{1}{r}\frac{\partial F}{\partial r} + \frac{\partial^2 F}{\partial r^2} - \frac{F}{r^2} = 0 \qquad (1.1a)$$

Differentiation of Eq. (1.2) with respect to r gives

$$\left(1-\frac{V^2}{c^2}\right)\frac{\partial^2}{\partial x^2}\left(\frac{\partial \phi_1}{\partial r}\right)+\frac{1}{r}\frac{\partial}{\partial r}\left(\frac{\partial \phi_1}{\partial r}\right)+\frac{\partial^2}{\partial r^2}\left(\frac{\partial \phi}{\partial r}\right)-\frac{1}{r^2}\left(\frac{\partial \phi_1}{\partial r}\right)=0 \quad (1.2a)$$

Comparing Eq. (1.1a) with Eq. (1.2a), it is easily seen that Eq. (1.4) is a solution of Eq. (1.1). The function f has to be determined by the boundary condition

$$v_0=\frac{1}{\cos\theta}\left(\frac{\partial \phi_2}{\partial r}\right)_{r=R}=-\alpha^2\int_{\cosh^{-1}\frac{x}{\alpha R}}^{0} f'(x-\alpha R\cosh u)\cosh^2 u\,du \quad (1.5)$$

where v_0 is the normal component of the velocity V of the undisturbed flow, and R is the radius of the body.

The complete solution of flow over an inclined body of revolution is then obtained by superimposing a cross-flow upon an axial flow, i.e.

$$\phi = \phi_1 + \phi_2$$

This solution was also suggested independently by C. Ferrari (Ref. 5).

From the velocity potential ϕ, one can calculate the pressure distribution over the body and then the aerodynamic forces. However, since the theory is based upon the linearized equation, the cross product terms of derivatives of ϕ_1 and ϕ_2 in the pressure calculation can be neglected.

Therefore the following simplification results: the resistance or drag can be calculated from the axial flow alone and the lift can be separately computed from the cross flow. Since the resistance was calculated before, (Ref.1), the following treatment is concerned only with the lift force. The lift acting in a direction perpendicular to the axis of the body and the moment about the vortex are thus

$$L = \int_0^{\pi}\int_0^{\infty} \Delta p \, r \, d\theta \cos\theta \, dx \approx 2\rho V \int_0^{\pi}\int_0^{\infty} \frac{\partial \phi_2}{\partial x} r \cos\theta \, d\theta \, dx$$

$$M = \int_0^{\pi}\int_0^{\infty} \Delta p \, r \, d\theta \cos\theta \, x \, dx \approx 2\rho V \int_0^{\pi}\int_0^{\infty} \frac{\partial \phi_2}{\partial x} x r \cos\theta \, d\theta \, dx \tag{1.6}$$

where Δp is the difference between the pressure at the surface of the body and that of the undisturbed flow and ρ is the density of the fluid in the undisturbed flow.

Eq. (1.5) is a non-homogeneous linear integral equation in f which does not have a general solution of simple form. However, it is interesting to see how Eq. (1.5) simplified in the limiting case when the radius of body approaches zero. It is convenient here to use $\xi = x - \alpha r \cosh u$ as the independent variable, then Eq. (1.5) becomes

$$v_0 = \frac{1}{R^2} \int_0^{x-\alpha R} \frac{f'(\xi)(x-\xi)^2 d\xi}{\sqrt{(x-\xi)^2 - \alpha^2 R^2}} \approx \frac{1}{R^2} \int_0^{x-\alpha R} f'(\xi)(x-\xi) d\xi$$

Integrating by parts, one has

$$v_0 \approx \frac{1}{R^2}\left\{ \Big[f(\xi)(x-\xi) \Big]_0^{x-\alpha R} + \int_0^{x-\alpha R} f(\xi)\, d\xi \right\}$$

Now, if the projectile is pointed nose, the doublet strength must be zero at the nose $x = 0$, thus $f(0) = 0$. Let $R \to 0$, and writing x instead of ξ in the integrand the above equation reduces to

$$v_0 \approx \frac{1}{R^2} \int_0^x f(x)\, dx \tag{1.5a}$$

Since the cross-sectional area of the body of revolution is $S = \pi R^2$, Eq. (1.5a) can be written as

$$v_0 = \frac{\pi}{S} \int_0^x f(x)\, dx$$

or

$$\int_0^x f(x)\, dx = \frac{v_0}{\pi} S$$

Differentiating, one arrives at

$$f(x) = \frac{v_0}{\pi} \frac{dS}{dx} \tag{1.7}$$

In order to calculate the lift, one has first to find the axial component of disturbance velocity. Thus

$$\left(\frac{\partial \phi_2}{\partial x}\right)_{r=R} = -\alpha \cos\theta \int_{\cosh^{-1}\frac{x}{\alpha R}}^{0} f'(x - \alpha R \cosh u) \cosh u \, du$$

$$= \frac{\cos\theta}{R} \int_0^{x-\alpha R} \frac{f'(\xi)(x-\xi)\,d\xi}{\sqrt{(x-\xi)^2 - \alpha^2 R^2}}$$

$$\approx \frac{\cos\theta}{R} \int_0^{x} f'(\xi)\,d\xi = \frac{\cos\theta}{R} f(x) = \frac{v_0 \cos\theta}{\pi R} \frac{dS}{dx}$$

Substituting into Eq. (1.6), the lift force is obtained as

$$L = 2\rho V \int_0^{\pi} \int_0^{\infty} \frac{v_0 \cos^2\theta}{\pi} \frac{dS}{dx} \, d\theta \, dx = \rho_0 V v_0 A_b$$

Where A_b = area of the base section of the body.

Hence the lift coefficient can be evaluated as

$$C_L = \frac{L}{\frac{\rho}{2} V^2 A_b} = 2 \frac{v_0}{V} \approx 2 \psi \qquad (1.8)$$

in which ψ = angle of attack of the body.

The moment arm d, i.e., the distance between the point of application of the resultant lift force and the vertex can be obtained by dividing the moment computed from

Eq. (1.6) by the lift force, and thus

$$d = \left(\frac{A_b - A_m}{A_b}\right) l \tag{1.9}$$

where $A_m =$ area of the mean section of the body, i.e., the volume of the body divided by its length, l.

The results of Eq. (1.8) and Eq. (1.9) are identical to those found in Munk's theory of airships (Ref. 6). At first sight, this might be surprising. However, if the radius of the body approaches zero as assumed, the cross-flow pattern is the same as that for an infinitely long circular cylinder moving with its axes perpendicular to the flow. Therefore, in every plane perpendicular to the axis of the body, the flow can be considered as two dimensional, i.e., it is independent of the variable x. Hence Eq. (1.1) reduces simply to

$$\frac{\partial^2 \phi}{\partial r^2} + \frac{1}{r}\frac{\partial \phi}{\partial r} + \frac{1}{r^2}\frac{\partial^2 \phi}{\partial \theta^2} = 0 \tag{1.1b}$$

This is immediately recognized as the equation of motion for two dimensional flow of incompressible fluids, which is the basis of Munk's theory.

Due to this two dimensional character of the flow, the distribution of doublets is not affected by the change in Mach's number, which is only connected with the independent

variable χ , and, therefore, the lift coefficient and the moment arm are also independent of Mach's number as shown by Eq. (1.8) and Eq. (1.9). This can also be seen from the fact that when r approaches zero, the variable $\xi = \chi - \alpha r \cosh u \rightarrow \chi$ and thus the effect of α , which is a function of Mach's number, is removed. To study the effect of Mach's number on the lift of the body, one has to go back to Eq. (1.5). To avoid the difficulty of solving this integral equation, the "indirect method" of solution can be employed, i.e., take a function f and determine the necessary shape of the body to comply with this function f.

Taking the simplest case

$$f(\chi - \alpha r \cosh u) = K(\chi - \alpha r \cosh u)$$

where K = a constant. Then

$$\phi_2 = -K\alpha\cos\theta \int_{\cosh^{-1}\frac{\chi}{\alpha r}}^{0} (\chi - \alpha r\cosh u)\cosh u\, du$$

$$= K\alpha\cos\theta \left\{ \frac{\chi}{2}\sqrt{\left(\frac{\chi}{\alpha r}\right)^2 - 1} - \frac{\alpha r}{2}\cosh^{-1}\frac{\chi}{\alpha r} \right\}$$

And the boundary condition reduces to

$$V_0 = \frac{K\alpha^2}{2}\left\{ \left(\frac{\chi}{\alpha R}\right)\sqrt{\left(\frac{\chi}{\alpha R}\right)^2 - 1} + \cosh^{-1}\left(\frac{\chi}{\alpha R}\right) \right\}$$

Therefore, the solution, Eq. (1.4a), is evidently a solution for a cone with half vertex angle ϵ , if $\cot\epsilon = \frac{\chi}{R}$. By putting $\frac{\cot\epsilon}{\alpha} = \zeta$ the boundary condition can

be written in the form

$$v_0 = \frac{\alpha^2 K}{2}\left\{\zeta\sqrt{\zeta^2-1} + \cosh^{-1}\zeta\right\} \qquad (1.5b)$$

For any given value of vertex angle and Mach's number, the corresponding value of K can be obtained from Eq. (1.5b)

In order to calculate the lift, one has first to find the axial component of disturbance velocity. Thus from Eq. (1.4a)

$$\left(\frac{\partial\phi_2}{\partial x}\right)_{r=R} = \frac{\alpha K\cos\theta}{2}\left[\sqrt{\left(\frac{x}{\alpha R}\right)^2-1} + \frac{\left(\frac{x}{\alpha R}\right)^2}{\sqrt{\left(\frac{x}{\alpha R}\right)^2-1}} - \frac{1}{\sqrt{\left(\frac{x}{\alpha R}\right)^2-1}}\right]$$

$$= \alpha K\cos\theta\sqrt{\zeta^2-1}$$

Substituting into Eq. (1.6), the lift force is found to be

$$L = 2\rho V v_0\int_0^{\pi}\int_0^{\infty}\frac{\partial\phi_2}{\partial x}\, r\cos\theta\, d\theta\, dx$$

$$= \frac{\alpha K\sqrt{\zeta^2-1}\;\rho V}{2}\int_0^{\infty}2\pi r\, dx$$

$$= \frac{\alpha K\sqrt{\zeta^2-1}\;\rho V\cos\epsilon}{2}\, S$$

where $S =$ lateral surface area of the cone. Therefore

$$C_L = \frac{L}{\frac{\rho}{2}V^2 A_b} = \frac{\alpha k \sqrt{\zeta^2-1}}{v_0} \cot \varepsilon \cdot \psi$$

But from Eq. (1.5b), k is obtained as

$$k = \frac{2 v_0}{\alpha^2 \{\zeta\sqrt{\zeta^2-1} + \cosh^{-1}\zeta\}}$$

Hence $\quad C_L = K_1 \psi \qquad (1.10)$

where $$K_1 = \frac{2\zeta\sqrt{\zeta^2-1}}{\zeta\sqrt{\zeta^2-1} + \cosh^{-1}\zeta}$$

In the limiting case when ϵ approached zero,

$$K_1 \longrightarrow 2$$

which agrees with Eq. (1.8). Similarly from Eq. (1.6) the moment coefficient is

$$C_M = \frac{\text{moment about vertex}}{\frac{\rho}{2} V^2 A_b \ell} = \frac{2}{3} K_1 \psi \qquad (1.11)$$

which satisfies Eq. (1.9).

Both Eq. (1.8) and Eq. (1.10) show that the lift at a given Mach's number is proportional to the angle of attack of the

body. This is a general characteristic of flow around a body without separation. If the fluid separates from the body and creates a "dead water" region on lee side of the body, then the lift will be proportional to the square of the angle of attack as was shown by W. Bollay (Ref. 7). The problem whether the fluid separates or not can only be answered by experiments. From the experimental data now available, (Ref. 8), it seems that the flow is continuous without separation, and, therefore, the lift is proportional to the angle of attack of the body.

Fig. 1.2 is the result of computation using Eq. (1.10). Calculations were carried out for values of $K_1 \geqq 1$, because the value of $K_1 = 1$ corresponds to $\epsilon = \beta$, where β is the wave angle. For $K_1 < 1$ it is found that $\beta < \epsilon$. This means that the wave angle is smaller than the vertex angle which is, of course, impossible. Therefore, $K_1 = 1$ marks the limit of validity of this solution. In fact, even when K_1 is near to 1, the solution must be considered as qualtitave only, since in this region the effect of the surface of the body on the shock wave cannot be neglected.

To generalize the solution for a body of revolution with a sharp point at the origin and cylindrical shape at infinity, it is simplest to use a step-wise doublet distribution. Consider the points $P_1, P_2, \cdots\cdots, P_n, \cdots P_N$ of the

meridian line of the body, and designate their co-ordinates by $x_1, R_1;\ x_2, R_2;\ \cdots\cdots;\ x_n R_n;\ \cdots;\ x_N, R_N$ and the corresponding values of $x - \alpha R$ by $\xi_1, \xi_2, \cdots \xi_n, \cdots\cdots \xi_N$

Then the boundary condition of Eq. (1.5) can be written as

$$v_0 = -\frac{\alpha^2}{2}\sum_{i=1}^{n} K_i \left\{ \left(\cosh^{-1}\frac{x_n - \xi_{i-1}}{\alpha R_n} - \cosh^{-1}\frac{x_n - \xi_i}{\alpha R_n} \right) + \left(\frac{x_n - \xi_{i-1}}{\alpha R_n}\sqrt{\left(\frac{x_n - \xi_{i-1}}{\alpha R_n}\right)^2 - 1} - \frac{x_n - \xi_i}{\alpha R_n}\sqrt{\left(\frac{x_n - \xi_i}{\alpha R_n}\right)^2 - 1} \right) \right\} \tag{1.5c}$$

This condition actually gives a set of N equations to determine the N constants K_i. This set of equations can be solved rather easily because each following equation in the set only contains one more which does not appear in the preceding one of the set. When K_i's are determined, the lift can be calculated by using Eq. (1.6). The pressure over each section of the conical surface is constant. The lift and moment coefficients are thus obtained as

$$C_L = \frac{2\psi}{\alpha}\sum_{n=0}^{n=N} \frac{(x_{n+1} - x_n)}{R_N}\frac{(R_{n+1} + R_n)}{R_N}\left\{ \sum_{i=0}^{i=n} K_i \left[\sqrt{\left(\frac{x_n - \xi_{i-1}}{\alpha R_n}\right)^2 - 1} - \sqrt{\left(\frac{x_n - \xi_i}{\alpha R_n}\right)^2 - 1} \right] \right\}$$

$$C_M = \frac{2\psi}{\alpha l}\sum_{n=0}^{n=N} \left\{ \frac{x_{n+1} + 2x_n}{3} + \frac{(x_{n+1} - x_n)}{3}\left(\frac{R_{n+1}}{R_{n+1} + R_n}\right) \right\} \frac{(x_{n+1} - x_n)}{R_N}\left(\frac{R_{n+1} + R_n}{R_N}\right) \left\{ \sum_{i=0}^{i=n} K_i \left[\sqrt{\left(\frac{x_n - \xi_{i-1}}{\alpha R_n}\right)^2 - 1} - \sqrt{\left(\frac{x_n - \xi_i}{\alpha R_n}\right)^2 - 1} \right] \right\} \tag{1.12}$$

where P_N is the last point on the meridian line, R_N is the base radius and ℓ is length of the body.

Fig. 2.3 is the result of the calculation using Eq. (2.12) for a body of revolution with "6-cliber head" and total length of 4.8 calibers, when it is travelling with a velocity 2.69 times that of sound (α = 2.5). The lift coefficient is considerably higher than that of a cone at the same angle of attack and at the same Mach's number, evidently due to the cylindrical part of the body. The position of the resulting lift force is also shown in the figure. Since, as mentioned before, lift and drag are independent in first order approximation, the calculated lift coefficient can be combined with the drag coefficient taken from experiments and thus give some information on the magnitude and direction of the resulting force. Fig. 2.4 shows the method applied to this projectile with the drag coefficient taken from Kent's experiment (Ref. 9).

If the projectile has a length of 4.34 diameters instead of 4.8 diameters and has the same nose shape, and, if its center of gravity is located at a point 2.68 diameters back of the nose, then the calculated moment about the center of gravity can be expressed as $M = \rho V^2 R_N{}^3 \psi f(\frac{V}{c})$ where $f(\frac{V}{c}) = 9.35$ for $\frac{V}{c} = 2.69$.
This compares closely with the value $f(\frac{V}{c}) = 10.7$ extrapolated from R. H. Fowler's experiment (Ref. 8), for a

projectile of the same proportions. This shows that the theory developed in this paper can be applied to a projectile with fair accuracy.

REFERENCES ON PART (II)

1. Th. von Karman and N. B. Moore: "The Resistance of Slender Bodies Moving with Supersonic Velocities with Special Reference to Projectiles", Tans. ASME Vol. 54, pp. 303-310, 1932.

2. G. I. Taylor and J. W. Maccoll: "The Air Pressure on a Cone Moving at High Speeds", Proc. Royal Society (A), Vol. 139, pp. 278-298, 1933.
J. W. Maccoll: "The Conical Shock Wave formed by a Cone moving at a High Speed", Proc. Royal Society (A), Vol. 159, pp. 459-472, 1937. The comparison was mentioned in a paper by G. I. Taylor: "Well Established Problems in High Speed Flow", Atti dei V Convengo "Volta": "Le alte velocita in aviazione", pp. 198-214, 1936, Reale Accademia d'Italia, Rome.

3. Levi-Civita: "Nuovo Cimento" (4), Vol. 6, 1897.

4. H. Lamb: "On Wave-Propagation in Two Dimensions", Proc. London Math. Society (1), Vol. 35, p. 141, 1902. See also H. Lamb: "Hydrodynamics", p. 298, 6th Ed., Cambridge 1932.

5. C. Ferrari: "Campi di corrente ipersonora attorno a solidi di rivoluzione", L'Aerotecnica, Vol. 17, fasc. 507-518, 1937,

6. M. M. Munk: "The Aerodynamic Forces on Airship Hulls", NACA Technical Report No. 184, 1934.

7. W. Bollay: "A Theory for Rectangular Wings of Small Aspect Ratio", Jour. Aeronautical Sciences, Vol. 4, p. 294-296, 1937.

8. R. H. Fowler, E. G. Gallop, C. N. H. Lock and H. W. Richmond: "The Aerodynamics of a Spinning Shell", Philosophical Trans. of Royal Society of London (A), Vol. 221, pp. 295-389. 1921.

9. K. M. Kent: "The Rôle of Model Experiments in Projectile Design", Mechanical Engineering, Vol 54, pp. 641-646, 1932.

PART (III)

APPLICATION OF TSCHAPLIGIN'S TRANSFORMATION TO

TWO DIMENSIONAL SUBSONIC FLOW

The equations of two dimensional irrotational motion of compressible fluids, assuming that the pressure is a single-valued function of density only, can be reduced to a single non-linear equation of the velocity potential. In the supersonic case, the problem is solved by Prandtl, Meyer and Busemann by means of the powerful method of characteristics. The essential difficulty of this problem lies in the subsonic case especially when the velocity is near to the velocity of sound. The first logical step is to linearize the equation based on the argument that the disturbance super-imposed on the parallel rectilinear flow due to the presence of a solid body is sufficiently small compared with parallel flow. This makes the second and higher order terms of disturbance potential to be negligible. An example of this method is the well-known theory of thin airfoil due to Prandtl and Glauert. But the presence of stagnation point at the nose of the airfoil makes the application of the linearized theory questionable, at least near this region; because there the disturbance due to the presence of the body is no longer small. On the same ground, the theory breaks down in case of

bodies whose dimension across the stream is not small compared with the dimension parallel to the stream. The next method is that derived originally by Janzen and Lord Rayleigh. They solved the equation by successive approximations. However, the process is very tedious and the method convergent very slowly if the velocity approaches that of sound.

Molenbroeck (Ref. 1) and Tschapligin (Ref. 2) suggested the use of the magnitude of velocity and inclination of velocity to the x-axis as independent variables and were able thus to reduce the equation of velocity potential to a linear equation. This equation was solved by Tschapligin (Ref. 2) and recently put in a more convenient form by F. Clauser and M. Clauser (Ref. 3). The solution is essentially a series each term of which is a product of hypergeometric function and circular function. The chief difficulty in practical application of this solution is to obtain a proper set of boundary conditions in the transformed plane, or the hodograph plane.

Tschapligin (Ref. 2) showed that a great simplification of the equation in hodograph plane results if the ratio of specific heats of the gas is equal to -1. Then the equation becomes the equation of minimal surface whose solution is well-known. However, at first, the hypothetical value of ratio of specific heats (all real gas has the value for this ratio ranging from 1.00 to 2.00) makes the practical application of

Tschapligin's theory questionable. It was Demtschenko (Ref. 4) and Busemann (Ref. 5) who made the meaning of this special value of ratio clear. They found that this special value of ratio of specific heats really corresponds to take the tangent of $p-v$ curve of gas instead $p-v$ curve itself. However, they limit themselves to use the tangent at the state of rest of the gas. Thus their theory can only apply to velocities up to o.5 times sound velootiy. In this part , the theory is generalized to use the tangent at the state of gas corresponding to the undisturbed parallel flow. Therefore the range of usefulness of the theory is greatly extended. In the first section, the general theory will be developed. In the second section, the theory will be applied to the case of symmetrical Joukowsky airfoil at zero angle of attack.

Section (I)

If p is the pressure and $1/v$ is the density of gas, the adiabatic process is expressed as a curve in the p-v plane as shown in Fig. 3.1. Now conditions near to the point p_1, v_1 can be approximated by the tangent at this point. The equation of the tangent at this point can be written as

$$p_1 - p = C(v_1 - v) = C(\rho_1^{-1} - \rho^{-1}) \quad (3.1)$$

where ρ is the density of the gas. Now the slope C

must be equal to the slope of the curve at the point p_1, v_1

$$C = \left(\frac{dp}{dv}\right)_1 = \left(\frac{dp}{d\rho}\frac{d\rho}{dv}\right)_1 = -\left(\frac{dp}{d\rho}\right)_1 \rho_1^2 = -a_1^2\rho_1^2$$

Therefore $\quad C = -a_1^2\rho_1^2$

Hence the approximate $p-\rho$ relation near p_1, ρ_1 can be written as

$$p_1 - p = a_1^2\rho_1^2\left(\frac{1}{\rho} - \frac{1}{\rho_1}\right) \tag{3.2}$$

From the generalized Bernoulli's theorem, the following relation is obtained

$$\frac{1}{2}w_2^2 - \frac{1}{2}w_3^2 = \int_2^3 \frac{dp}{\rho} \tag{3.3}$$

where w is the velocity of gas, the subscripts $2, 3$ indicate two conditions. But from Eq. (3.2), p can be expressed as a function of ρ, thus

$$dp = \frac{a_1^2\rho_1^2}{\rho^2}\,d\rho \tag{3.4}$$

Substituting into the integrand in Eq. (3.3) and integrate, the following relation is obtained

$$\frac{1}{2}w_2^2 - \frac{1}{2}w_3^2 = \frac{1}{2}a_1^2\rho_1^2\left\{\frac{1}{\rho_3^2} - \frac{1}{\rho_2^2}\right\}$$

Now if $w_3 = 0$, $w_2 = w$, $\rho_3 = \rho_0$ and $\rho_2 = \rho$, then

$$\frac{a_1^2 \rho_1^2}{\rho_0^2} + w^2 = \frac{\rho_1^2 a_1^2}{\rho^2} \qquad (3.5)$$

where the subscript 0 denotes the rest state of the gas. If the sound velocity a is defined as the derivative of p with respect to ρ, then Eq. (3.4) gives

$$\frac{dp}{d\rho}\rho^2 = a^2\rho^2 = a_1^2\rho_1^2 = \text{constant} \qquad (3.6)$$

Therefore Eq. (3.5) can be written as

$$\left(\frac{\rho}{\rho_0}\right)^2 = 1 - \frac{w^2}{a^2}$$

or

$$\frac{\rho}{\rho_0} = \sqrt{1 - \frac{w^2}{a^2}} \qquad (3.7)$$

Furthermore, from Eq. (3.6), $\rho_1^2 a_1^2 = \rho_0^2 a_0^2$, thus Eq. (3.7) can also be written as

$$\frac{\rho_0}{\rho} = \sqrt{1 + \frac{w^2}{a_0^2}} \qquad (3.8)$$

It is interesting at this stage, to notice that from Eq. (3.8), the density decreases as velocity w increases, as it is expected. Thus from Eq. (3.7), the velocity of sound of the gas will increase as the velocity is

increased. This is just opposite to real gas, because in the case of an adiabatic flow, it is well-known that the temperature of gas decreases as the velocity of gas is increased and thus the sound velocity also decreases. However from Eq. (3.7), the ratio $\frac{w}{a}$ or Mach's number increases as the velocity w increases. But this ratio only reaches the value unity when $w = \infty$, or from Eq. (3.8) when $\rho = 0$. It is thus seen that the entire region of flow is subsonic and thus the equation of motion is always of elliptic type. This may be considered as the physical reason why the complex representation of velocity potential and stream function is possible in all cases, as will be shown in following pages. However one should bear in mind that the portion of tangent that could be used as an approximation to the true adiabatic curve, must lie within the first quadrant. Thus the upper limit of velocity for practical application of the theory is when $p = 0$. By using Eqs. (3.2), (3.7) and (3.8), this upper limit is found to be

$$\left(\frac{w}{w_1}\right)_{max.} = \frac{1}{\left(\frac{w_1}{a_1}\right)} \sqrt{\left(\frac{p_1}{\rho_1 a_1^2} + 1\right)^2 - \left(1 - \frac{w_1^2}{a_1^2}\right)}$$

Or by putting $a_1^2 = \gamma \frac{p_1}{\rho_1}$, the above equation reduces to

$$\left(\frac{w}{w_1}\right)_{max.} = \frac{1}{\left(\frac{w_1}{a_1}\right)} \sqrt{(\gamma+1)^2 - \left\{1 - \left(\frac{w_1}{a_1}\right)^2\right\}}$$

The values of $\left(\frac{w}{w_1}\right)_{max.}$ for different values of $\frac{w_1}{a_1}$ are shown in Table 3.1.

Table 3.1

$\frac{w_1}{a_1}$	$\left(\frac{w}{w_1}\right)_{max.}$	$\left(\frac{w}{a_1}\right)_{max.}$
0	∞	2.186
0.2	10.91	2.195
0.4	5.56	2.225
0.6	3.78	2.265
0,8	2.92	2.335
1.0	2.405	2.405

It is thus seen that for most applications of this theory, p will remain positive. However due to large deviation from the true adiabatic process at high values of $\frac{w}{w_1}$, one has probably to limit the ratio $\left(\frac{w}{w_1}\right)$ to about 2.

Now if the flow is irrotational, there exists a velocity potential ϕ such that

$$\frac{\partial \phi}{\partial x} = u, \qquad \frac{\partial \phi}{\partial y} = v \tag{3.9}$$

where u, v are the x, y components of the velocity w. To satisfy the equation of continuity, the stream function ψ is introduced. It is defined by

$$\frac{\rho}{\rho_0} u = \frac{\partial \psi}{\partial y}, \qquad \frac{\rho}{\rho_0} v = -\frac{\partial \psi}{\partial x} \tag{3.10}$$

Now if the angle of inclination of the velocity w to the x-axis is β, then from Eqs. (3.9) and (3.10), one has

$$\begin{aligned} d\phi &= w \cdot \cos\beta \, dx + w \cdot \sin\beta \, dy \\ d\psi &= -w \frac{\rho}{\rho_0} \sin\beta \, dx + w \frac{\rho}{\rho_0} \cos\beta \, dy \end{aligned} \tag{3.11}$$

Solving for dx and dy,

$$\begin{aligned} dx &= \frac{\cos\beta}{w} d\phi - \frac{\sin\beta}{w} \frac{\rho_0}{\rho} d\psi \\ dy &= \frac{\sin\beta}{w} d\phi + \frac{\cos\beta}{w} \frac{\rho_0}{\rho} d\psi \end{aligned} \tag{3.12}$$

So long as the correspondence between the physical plane and the hodoplane is one to one, or mathematically $\frac{\partial(x, y)}{\partial(u, v)} \neq 0$ one can express x, y as functions of w, β and so also ϕ and ψ as functions w and β. Thus

$$d\phi = \phi'_w \, dw + \phi'_\beta \, d\beta$$
$$d\psi = \psi'_w \, dw + \psi'_\beta \, d\beta \qquad (3.13)$$

where primes indicate the derivative, and subscript indicate the variables with respect to which the functions are differentiated. Now substitute Eq. (3.13) into Eq. (3.12), the following relations are obtained

$$dx = \left(\frac{\cos\beta}{w} \phi'_w - \frac{\sin\beta}{w} \frac{\rho_0}{\rho} \psi'_w \right) dw + \left(\frac{\cos\beta}{w} \phi'_\beta - \frac{\sin\beta}{w} \frac{\rho_0}{\rho} \psi'_\beta \right) d\beta$$
$$(3.14)$$
$$dy = \left(\frac{\sin\beta}{w} \phi'_w + \frac{\cos\beta}{w} \frac{\rho_0}{\rho} \psi'_w \right) dw + \left(\frac{\sin\beta}{w} \phi'_\beta + \frac{\cos\beta}{w} \frac{\rho_0}{\rho} \psi'_\beta \right) d\beta$$

Since the left-hand sides of Eq. (3.14) are exact differential, one can apply the reciprocity relation and obtains

$$\frac{\partial}{\partial\beta} \left(\frac{\cos\beta}{w} \phi'_w - \frac{\sin\beta}{w} \frac{\rho_0}{\rho} \psi'_w \right) = \frac{\partial}{\partial w} \left(\frac{\cos\beta}{w} \phi'_\beta - \frac{\sin\beta}{w} \frac{\rho_0}{\rho} \psi'_\beta \right)$$
$$(3.15)$$
$$\frac{\partial}{\partial\beta} \left(\frac{\sin\beta}{w} \phi'_w + \frac{\cos\beta}{w} \frac{\rho_0}{\rho} \psi'_w \right) = \frac{\partial}{\partial w} \left(\frac{\sin\beta}{w} \phi'_\beta + \frac{\cos\beta}{w} \frac{\rho_0}{\rho} \psi'_\beta \right)$$

Carrying out the differentiation, and cancelling identical terms in left-hand and right-hand side,

$$-\frac{\sin\beta}{w} \phi'_w - \frac{\cos\beta}{w} \frac{\rho_0}{\rho} \psi'_w = -\frac{\cos\beta}{w^2} \phi'_\beta + \frac{\sin\beta}{w^2} \frac{\rho_0}{\rho} \left(1 - \frac{w^2}{a^2}\right) \psi'_\beta$$
$$(3.16)$$
$$\frac{\cos\beta}{w} \phi'_w - \frac{\sin\beta}{w} \frac{\rho_0}{\rho} \psi'_w = -\frac{\sin\beta}{w^2} \phi'_\beta - \frac{\cos\beta}{w^2} \frac{\rho_0}{\rho} \left(1 - \frac{w^2}{a^2}\right) \psi'_\beta$$

Using Eq. (3.7), Eq. (3.16) becomes

$$-\frac{\sin\beta}{w}\phi_w' - \frac{\cos\beta}{w}\frac{\rho_0}{\rho}\psi_w' = -\frac{\cos\beta}{w^2}\phi_\beta' + \frac{\sin\beta}{w^2}\frac{\rho}{\rho_0}\psi_\beta'$$

$$\frac{\cos\beta}{w}\phi_w' - \frac{\sin\beta}{w}\frac{\rho_0}{\rho}\psi_w' = -\frac{\sin\beta}{w^2}\phi_\beta' - \frac{\cos\beta}{w^2}\frac{\rho}{\rho_0}\psi_\beta' \tag{3.17}$$

As in both equations ϕ_w', ψ_w', and ϕ_β', ψ_β' are connected with a proportional factor, one can solve for them, and

$$\begin{aligned}\phi_w' &= -\frac{\rho}{\rho_0}\frac{1}{w}\psi_\beta' \\ \phi_\beta' &= \frac{\rho_0}{\rho}w\,\psi_w'\end{aligned} \tag{3.18}$$

Now Eq. (3.18) can be further reduced if a new variable ω is introduced. ω is defined as

$$d\omega = \frac{\rho}{\rho_0}\frac{dw}{w} \tag{3.19}$$

Then Eq. (3.18) becomes

$$\begin{aligned}\phi_\omega' &= -\psi_\beta' \\ \phi_\beta' &= \psi_\omega'\end{aligned} \tag{3.20}$$

This is the fundamental set of equations for the present theory. It can be easily recognized as the Cauchy-Riemann differential equation, and thus $\phi + i\psi$ must be an analytic function of $\beta + i\omega$. However for the convenience of numerical calculation, a new variable W is used instead of ω, such that

$$W = a_0 \cdot e^{\omega} \tag{3.21a}$$

Or by integrating Eq. (3.19),

$$W = \frac{2a_0 w}{\sqrt{a_0^2 + w^2} + a_0} \tag{3.21}$$

Hence by inverting,

$$w = \frac{4a_0^2 W}{4a_0^2 - W^2} \tag{3.22}$$

Thus by substituting into Eq. (3.8),

$$\frac{\rho_0}{\rho} = \frac{4a_0^2 + W^2}{4a_0^2 - W^2} \tag{3.23}$$

If another set of new variables $U = W\cos\beta$ and $V = W\sin\beta$ are used as independent variables, one has

$$\frac{\partial}{\partial \omega} = \frac{\partial U}{\partial \omega}\frac{\partial}{\partial U} + \frac{\partial V}{\partial \omega}\frac{\partial}{\partial V} = W\left\{\cos\beta\frac{\partial}{\partial U} + \sin\beta\frac{\partial}{\partial V}\right\}$$

$$\frac{\partial}{\partial \beta} = \frac{\partial U}{\partial \beta}\frac{\partial}{\partial U} + \frac{\partial V}{\partial \beta}\frac{\partial}{\partial V} = W\left\{-\sin\beta\frac{\partial}{\partial U} + \cos\beta\frac{\partial}{\partial V}\right\} \quad (3.24)$$

Using Eq. (3.24), Eq. (3.20) can be written as

$$\cos\beta\frac{\partial\phi}{\partial U} + \sin\beta\frac{\partial\phi}{\partial V} = \sin\beta\frac{\partial\psi}{\partial U} - \cos\beta\frac{\partial\psi}{\partial V}$$

$$-\sin\beta\frac{\partial\phi}{\partial U} + \cos\beta\frac{\partial\phi}{\partial V} = \cos\beta\frac{\partial\psi}{\partial U} + \sin\beta\frac{\partial\psi}{\partial V}$$

These equations are satisfied by

$$\frac{\partial\phi}{\partial U} = \frac{\partial\psi}{\partial(-V)}, \quad \frac{\partial\phi}{\partial(-V)} = -\frac{\partial\psi}{\partial U} \quad (3.25)$$

These are the Cauchy-Riemann differential equations, therefore the complex potential $F = \phi + i\psi$ is a function of $U - iV = \bar{W}$. Or.

$$\phi + i\psi = F(U - iV) = F(\bar{W})$$

Hence

$$\phi - i\psi = \bar{F}(U + iV) = \bar{F}(W) \quad (3.26)$$

To transform from hodograph plane back to physical plane, the expression of x and y in terms of U and V must be found. By using Eqs. (3.22) and (3.23), Eq. (3.12) can be written as

$$dx = \frac{U \cdot d\phi}{W^2}\left\{1 - \frac{W^2}{4a_0^2}\right\} - \frac{V \cdot d\psi}{W^2}\left\{1 + \frac{W^2}{4a_0^2}\right\}$$

$$dy = \frac{V\, d\phi}{W^2}\left\{1 - \frac{W^2}{4a_0^2}\right\} + \frac{U \cdot d\psi}{W^2}\left\{1 + \frac{W^2}{4a_0^2}\right\}$$

where $W^2 = U^2 + V^2$. These equations can be combined into one equation by means of Eq. (3.26). Thus

$$dz = dx + i\,dy = \frac{dF}{\bar{W}} - \frac{W \cdot d\bar{F}}{4a_0^2} \qquad (3.27)$$

For practical application of the theory to the flow over an obstacle, the computation proceeds as follows: (1) Find the complex potential for the flow of incompressible fluid over the obstacle, say

$$w_1 \cdot G(\xi + i\eta) = w_1\, G(\zeta)$$

where w_1 , is the velocity of parallel rectilinear undisturbed flow, and ξ , η the space coordinate of the physical plane. (2) Now let $F = W_1\, G(\zeta)$. Here W_1 is the

transformed undisturbed velocity, to be interpreted as Eq. (3.21). But the complex variable ζ has no direct physical meaning. (3) Using the above value of F, Eq. (3.27) can be written as

$$dz = d\zeta - \frac{1}{4}\left(\frac{W_1}{a_0}\right)^2 \left(\frac{d\bar{F}}{d\bar{\zeta}}\right)^2 d\bar{\zeta}$$

Integrating,

$$z = \zeta - \frac{1}{4}\left(\frac{W_1}{a_0}\right)^2 \int \left(\frac{d\bar{F}}{d\bar{\zeta}}\right)^2 d\bar{\zeta} \qquad (3.28)$$

Thus it is seen that the complex coordinate in the physical plane of compressible fluid is equal to the corresponding complex coordinate in the physical plane of incompressible fluid plus a correction term. The factor before the integral depends upon the Mach's number of the undisturbed flow only. By using Eqs. (3.7) and (3.8), and (3.21), one has

$$\frac{1}{4}\left(\frac{W_1}{a_0}\right)^2 = \frac{\left(\frac{w_1}{a_1}\right)^2}{\left\{1 + \sqrt{1 - \left(\frac{w_1}{a_1}\right)^2}\right\}^2} \qquad (3.29)$$

The integration constant of the integral in Eq. (3.28) is not important, because it only means a translation of the whole z - plane. (4) The velocity w corresponds to z can be computed by starting with

$$\bar{W} = \frac{dF}{d\zeta} = W_1 \frac{dG}{d\zeta} = U - iV$$

By means of Eq. (3.29)

$$\frac{w}{w_1} = \frac{\frac{|W|}{W_1}}{\frac{w_1}{W_1}\left[1 - \frac{1}{4}\left(\frac{W_1}{a_0}\right)^2\left(\frac{|W|}{W_1}\right)^2\right]}$$

Thus by putting $w - w_1$, one obtains

$$\frac{w_1}{W_1} = \frac{1}{1 - \frac{1}{4}\left(\frac{W_1}{a_0}\right)^2}$$

Thus

$$\frac{w}{w_1} = \left\{1 - \frac{1}{4}\left(\frac{W_1}{a_0}\right)^2\right\} \frac{\frac{|W|}{W_1}}{1 - \frac{1}{4}\left(\frac{W_1}{a_0}\right)^2\left(\frac{|W|}{W_1}\right)^2} \tag{3.30}$$

Using Eqs. (3.30 and (3.29), the ratio $\frac{w}{w_1}$ can be calculated easily. (5) To determine the pressure acting on the surface of the body one has to use Eq. (3.2). With some manipulation, the following relation is obtained:

$$\frac{p - p_1}{\frac{1}{2}\rho_1 w_1^2} = \frac{2}{\left(\frac{w_1}{a_1}\right)^2}\left[1 - \frac{\rho_0}{\rho}\left(\frac{\rho_1}{\rho_0}\right)\right]$$

$$= \frac{2}{\left(\frac{w_1}{a_1}\right)^2}\left[1 - \sqrt{1 - \left(\frac{w_1}{a_1}\right)^2}\,\frac{\rho_0}{\rho}\right]$$

But

$$\frac{\rho_0}{\rho} = \sqrt{1 + \left(\frac{w}{w_1}\right)^2 \left(\frac{w_1}{a_0}\right)^2}$$

$$= \sqrt{1 + \left(\frac{w}{w_1}\right)^2 \frac{\left(\frac{w_1}{a_1}\right)^2}{1 - \left(\frac{w_1}{a_1}\right)^2}} \qquad (3.31)$$

Therefore

$$\frac{p - p_1}{\frac{1}{2}\rho_1 w_1^2} = \frac{2}{\left(\frac{w_1}{a_1}\right)^2}\left\{1 - \sqrt{1 + \left\{\left(\frac{w}{w_1}\right)^2 - 1\right\}\left(\frac{w_1}{a_1}\right)^2}\right\} \qquad (3.32)$$

Section (II)

In this section, the general theory developed in Section (I) is applied to the simple case of flow over a symmetrical Joukowsky airfoil at zero angle of attack. The complex potential in the circle-plane (see Fig. 3.2) is known to be

$$w_1\left\{(\mu - b) + \frac{a^2}{\mu - b}\right\} \qquad (3.33)$$

where a = radius of the airfoil circle, b = eccentricity of the airfoil circle. The relation between the airfoil plane and circle-plane is the well-known Joukowsky transformation

$$\zeta = \mu + \frac{1}{\mu} \qquad (3.34)$$

if the radius of the transforming circle is unity.

Now the starting point of the calculation is the function to find $W\,d\bar{F}$

$$W\,d\bar{F} = \frac{d\bar{F}}{d\bar{\xi}}\,\frac{d\bar{F}}{d\bar{\mu}}\,d\bar{\mu} = \frac{\left(\frac{d\bar{F}}{d\bar{\mu}}\right)^2}{\frac{d\bar{\xi}}{d\bar{\mu}}}\cdot d\bar{\mu}$$

Therefore $W\,d\bar{F} = W_1^2\left\{1-\frac{a^2}{(\bar{\mu}-b)^2}\right\}^2\left\{1+\frac{1}{2}\left(\frac{1}{\bar{\mu}-1}-\frac{1}{\bar{\mu}+1}\right)\right\}$

Thus the correction term in Eq. (3.28) is

$$\frac{1}{4a_0^2}\int W\,dF = \frac{1}{4}\left(\frac{W_1}{a_0}\right)^2\left\{I_1+I_2-I_3\right\} \qquad (3.35)$$

where $I_1 = \int\left\{1-\frac{2a^2}{(\bar{\mu}-b)^2}+\frac{a^4}{(\bar{\mu}-b)^4}\right\}d\bar{\mu}$

$$I_2 = \frac{1}{2}\int\left\{1-\frac{2a^2}{(\bar{\mu}-b)^2}+\frac{a^4}{(\bar{\mu}-b)^4}\right\}\frac{d\bar{\mu}}{(\bar{\mu}-1)}$$

$$I_3 = \frac{1}{2}\int\left\{1-\frac{2a^2}{(\bar{\mu}-b)^2}+\frac{a^4}{(\bar{\mu}-b)^4}\right\}\frac{d\bar{\mu}}{\bar{\mu}+1}$$

These integrals can be easily computed and simplified, noting that $a-b=1$. If $(\bar{\mu}-b)=ae^{i\theta}$ and $\lambda = \frac{a}{1-b}$

$$I_1 = a\left\{e^{i\theta} + 2e^{-i\theta} - \frac{1}{3}e^{-3i\theta}\right\}$$

$$I_2 = \frac{1}{2}\left\{\frac{1}{6} - e^{-i\theta} + \frac{1}{2}e^{-2i\theta} + \frac{1}{3}e^{-3i\theta} + \log(ae^{i\theta})\right\}$$

$$I_3 = \frac{1}{2}\left\{(1-\lambda^2)^2 \log a\left(e^{i\theta} + \frac{1}{\lambda}\right) + \lambda^2(2-\lambda^2)\log ae^{i\theta} + \lambda\ (1-\lambda^2)e^{-i\theta} + \frac{\lambda^2}{2}e^{-2i\theta} - \frac{\lambda}{3}e^{-3i\theta}\right\} \quad (3.36)$$

Separating the real and imaginary parts, and adding,

$$\begin{aligned} Rl\ (I_1 + I_2 - I_3) &= a\left(3\cos\theta - \frac{1}{3}\cos 3\theta\right) \\ &+ \frac{1}{2}\left\{\frac{(1-\lambda^2)^2}{2}\log\left(1 + \frac{1}{\lambda^2} + \frac{2\cos\theta}{\lambda}\right) + (\lambda^3 - 2\lambda - 1)\cos\theta \right. \\ &\left. + \frac{1}{2}(1-\lambda^2)\cos 2\theta + \frac{1}{3}(1+\lambda)\cos 3\theta\right\} \end{aligned} \quad (3.37)$$

$$\begin{aligned} Im\ (I_1 + I_2 - I_3) &= a\left(-\sin\theta + \frac{1}{3}\sin 3\theta\right) \\ &+ \frac{1}{2}\left\{(1 + 2\lambda - \lambda^3)\sin\theta - \frac{1}{2}(1-\lambda^2)\sin 2\theta \right. \\ &\left. - \frac{1}{3}\ (1+\lambda)\sin 3\theta - (1-\lambda^2)^2\tan^{-1}\frac{\sin\theta}{\cos\theta + \frac{1}{\lambda}} + (1-\lambda^2)^2\theta\right\} \end{aligned}$$

These give the correction term to x and y coordinates.

The transformed velocity W over the surface of

the airfoil can be easily found by means of graphical method (Ref. 6). Then the actual velocity and pressure can be computed by using Eqs. (3.22) and (3.32).

Fig. 3.3 shows the result of calculation for the case $\lambda = 1.20$ and $\frac{w_1}{a_1} = 0.550$. The nose of the airfoil is somewhat rounded by transforming into the case of compressible fluid. However, the pressure gradient is steeper, as would be expected. The main defect of this type of calculation is that during the transformation from incompressible flow to compressible flow, the shape of the body is also changed. To isolate the effect of compressibility of the fluid, it is necessary to bring back the original shape of the body. This is done by first deforming the original Joukowsky airfoil, such that the final profile after correction for compressibility is same as the original Joukowsky airfoil. The amount of deformation is obtained from the calculation assuming that the airfoil was a Joukowsky airfoil at start. That is the effect of deformation on the correction term of Eq. (3.28) is neglected. This is allowable because the quantity neglected is a second order quantity.

This deformation of Joukowsky airfoil can be carried out by using the method developed by von Karman and Trefftz (Ref. 7). However, for some practical reasons, the Karman-Trefftz method is somewhat modified:

Fig. 3.4a shows two airfoils, both having the same chord, one is Joukowsky airfoil desired and the other is the airfoil resulted from the first step calculation. Now apply the Joukowsky transformation to this figure, then the Joukowsky airfoil will become a circle C_1 while the other airfoil a near-circular shape C as shown in Fig. 3.4b. The desired deformed Joukowsky airfoil will appear like C_2 in this figure. The difference between C_2 and C_1 is just opposite and equal to that between C_1 and C. Now let C_2 be written as $\zeta_2 = r e^{i\theta}$. Obviously,

$$r = 1 + g(\theta) \tag{3.38}$$

where $g(\theta)$ wil be small compared with 1. The function which established the conformal transformation of the outside of this boundary C_2 into outside of the circle C_1 may be denoted by

$$\zeta_1 = \zeta_2 \left[1 + f(\zeta_2) \right] \tag{3.39}$$

where ζ_1, ζ_2 have their origin at the center and the absolute value of $f(\zeta_2)$ is again small compared with 1. Then it is shown (Ref. 7) that

$$g(\theta) + Re\left[f(\zeta_2) \right] = 0 \tag{3.40}$$

In order to calculate $f(\zeta_2)$ we develop the

function $g(\theta)$ in a Fourier series:

$$g(\theta) = \sum_{0}^{\infty} a_n \cos n\theta \tag{3.41}$$

Here only consine terms appear because the airfoil is symmetrical about the chord. One the other hand, the complex function $f(\zeta_2)$ has the form, for $|\zeta_2| > 1$:

$$f(\zeta_2) = \sum_{0}^{\infty} \frac{c_n}{\zeta_2^{\,n}} \tag{3.42}$$

Now put $\zeta_2 \approx e^{i\theta}$, then (3.40) is satisfied by

$$c_n = -a_n$$

Thus

$$f(\zeta_2) = -\sum_{0}^{\infty} \frac{a_n}{\zeta_2^{\,n}} \tag{3.43}$$

It can be easily seen that the velocity around the deformed Joukowsky airfoil can be calculated as

$$w = w_J \left| \frac{d\zeta_1}{d\zeta_2} \right| \tag{3.44}$$

where w_J = velocity around the Joukowsky airfoil.

Now from Eqs. (3.39 and (3.43),

$$\frac{d\zeta_1}{d\zeta_2} = 1 - \sum_0^\infty{}' \frac{a_n}{\zeta_2^n} + \sum_0^\infty{}' \frac{n a_n}{\zeta_2^n}$$

$$= \left\{1 + \sum_0^\infty{}' (n-1) a_n \cos n\theta\right\} - i \sum_0^\infty{}' (n-1) a_n \sin n\theta$$

Neglecting small quantities of second order, and noting Eq. (3.41),

$$\left|\frac{d\zeta_1}{d\zeta_2}\right| = 1 + \sum_0^\infty{}' (n-1)\, a_n \cos n\theta$$

$$= 1 + \sum_0^\infty{}' n a_n \cos n\theta - \sum_0^\infty{}' a_n \cos n\theta \qquad (3.45)$$

$$= 1 + \frac{d}{d\theta} \sum_1^\infty{}' a_n \sin n\theta - g(\theta)$$

A trial calculation shows that the convergence of the coefficients a_n is not very good. Therefore, one must avoid manipulation on the Fourier series as required by Eq. (3.45). This is possible because $-\sum_0^\infty{}' a_n \sin n\theta$ is known to mathematicians as the allied or conjugate series of $\sum_0^\infty{}' a_n \cos n\theta$. It is also known (Ref. 8) that if $g(\theta) = \sum_0^\infty{}' a_n \cos n\theta$

$$-\sum_1^\infty{}' a_n \sin n\theta = \frac{1}{2\pi} \int_0^\pi \frac{g(\theta+\xi) - g(\theta-\xi)}{\tan\frac{\xi}{2}} d\xi$$

Therefore

$$\frac{d}{d\theta}\sum_{1}^{\infty} a_n \sin n\theta = -\frac{1}{2\pi}\int_0^{\pi}\frac{g'(\theta+\xi)-g'(\theta-\xi)}{\tan\frac{\xi}{2}}\,d\xi$$

Integrating by parts,

$$-\frac{1}{2\pi}\left\{\left[\frac{g(\theta+\xi)+g(\theta-\xi)}{\tan\frac{\xi}{2}}\right]_0^{\pi}+\frac{1}{2}\int_0^{\pi}\frac{g(\theta+\xi)+g(\theta-\xi)}{\sin^2\frac{\xi}{2}}\,d\xi\right\}$$

$$= -\frac{1}{2\pi}\int_0^{\pi}\frac{\{g(\theta+\xi)-g(\theta)\}+\{g(\theta-\xi)-g(\theta)\}}{(1-\cos\xi)}\,d\xi$$

Hence Eq. (3.45) can be written as

$$\left|\frac{d\zeta_1}{d\zeta_2}\right| = 1-\frac{1}{2\pi}\int_0^{\pi}\frac{\{g(\theta+\xi)-g(\theta)\}+\{g(\theta-\xi)-g(\theta)\}}{1-\cos\xi}\,d\xi - g(\theta) \qquad (3.46)$$

The integral is evidently convergent for any continuous regular function $g(\theta)$, because then the integrand is always finite. Its evaluation can be done numerically.

Fig. 3.5 is the result of calculation for a Joukowsky airfoil with the thickness parameter $b = 0.20$, at two speeds, $\frac{w_1}{a_1}$ = 0.450 and 0.550. The suction peaks are considerably higher with higher speeds. Also the

positions of pressure peaks tend to move backward with increasing speed. Both are in agreement with the experimental results obtained by J. Stack (Ref. 9). The values of $(p-p_1)/\frac{1}{2}\rho_1 w_1^2$ for $\frac{w_1}{a_1} = 0.550$ and $\frac{w_1}{a_1} = 0.450$ at which real air will attain a velocity equal to the local sound velocity are equal to -1.653 and -2.755 respectively. It is thus seen that the effect of compressibility on pressure distribution is appreciable, even when nowhere the local sound velocity is reached. One should, however, bear in mind that the effect on the force coefficient of the airfoil will probably not be so marked as with the pressure distribution, because the resultant force on the airfoil is the algebraic difference of pressure force acting on two sides of the section.

APPENDIX TO PART (III)

COMPARISON WITH OTHER METHODS

In order to check the accuracy of the method developed in PART (III), the flow over a finite circular cylinder with its axis perpendicular to the direction of undisturbed flow is studied. The method exposed in Section (II) of PART (III) for correction of shape of body is used. The following is the result of calculation for velocity at the top of the circular section, compared with results by other methods [collected by E. Pistolesi (Ref. 10)].

$$\frac{w_1}{a_1} = 0.400$$

Method	$\frac{w}{w_1}$ at top of section
Part (III)	2.268
Rayleigh	2.206
Poggi	2.194
Taylor's Electric Analogy	2.188

$$\frac{w}{w_1} = 2.000 \text{ for incompressible fluid.}$$

Thus the present method gives a higher value. However, the flow over a cylinder is rather an extreme case. Because the difference between the velocities to be calculated and the

and the undisturbed velocity is large, and thus this approximate method involves larger than usual error.

REFERENCES ON PART (III)

1. P. Molenbroek: Über einige Bewegungen eines Gases bei Annahme eines Geschwindigkeitspotentials, Arch d. Mathem. u. Phys., Grünert Hoppe (1890), Reihe 2, Bd. 9, S. 157.

2. A. Tschapligin: Scientific Memoirs of the Univ. Moscow. (In Russian) (1902).

3. F. Clauser, M. Clauser: New Methods of Solving the Equations for the Flow of a Compressible Fluid, Unpublished Ph.D. Thesis at C.I.T. (1937).

4. B. Demtchenko: Sur les mouvements lents des fluides compressibles, Comptes Rendus, Vol. 194, p. 1218 (1932). Also, Variation de la résistance aux faibles vitesses sous l'influence de la compressibilité, Comptes Rendus, Vol. 194, p. 1720 (1932).

5. A. Busemann: Die Expansionsberichtigung der Kontraktionsziffer von Blenden, Forschung, Bd. 4, S. 186-187 (1933). Also, Hodographenmethode der Gasdynamik, Z.A.M.M. Bd. 12, S. 73-79 (1937).

6. W. F. Durand: Aerodynamic Theory Vol. 2, p. 71-74, 1st Ed., Julius Springer, Berlin (1935).

7. Th. von Karman, E. Trefftz: Potentialströmung dem gegebene Tragflachenquerschnitte, Z. F. M. Bd. 9, S. 111 (1918). Also, W. F. Durand: Aerodynamic Theory, Vol. 2, p.80-83 (1935).

8. G. H. Hardy, J. E. Littlewood: The Allied Series of a Fourier Series, Proc. of London Math. Soc. (2) Vol. 24, pp.211-246 (1925).

9. J. Stack: The Compressibility Burble, NACA Technical Note No. 543 (1935).

10. E. Pistolesi: La portanza alle alte velocita inferiori a quella del suono, Atti dei V. Convengo "Volta", fasc 300, (1936) Reale Accademia d'Italia, Rome.

PART (IV)

FLIGHT ANALYSIS OF A SOUNDING ROCKET WITH SPECIAL REFERENCE TO PROPULSION BY SUCCESSIVE IMPULSES

Introdution

In 1919 R. H. Goddard (Ref. 1) published the historically important paper which suggested the use of nitro-cellulose powder as a propellant for raising a sounding rocket to altitudes beyond the range of sounding balloons. To determine the feasibility of this propellant, a series of experiments had been carried out and it was found that thermal efficiency of 50% could be expected if the powder was exploded in a properly designed chamber and the resulting gases were allowed to escape at high velocity through an expanding nozzle. In 1931 R. Tilling used a mixture of potassium chlorate and naphthalene as propellant and actually reached an altitude of 6,600 feet. More recently, L. Damblanc (Re. 2) made static tests with a slow burning black powder and from these estimated that a height of 10,000 feet could be reached using a two-step arrangement. The results so far reported offer an incentive to further analysis.

The effect of decreasing gravitational acceleration on the maximum height reached by a rocket has been considered by A. Bartocci (Ref. 3). However, he assumes that the

rocket itself has a constant acceleration during powered flight. L. Breguet and R. Devillers (Ref. 4) also considered the effect of the variation of g. To simplify the analysis, they assumed that the acceleration of the rocket was equal to a constant multiple of g. Since the sounding rocket for practical reasons will be propelled by a nearly constant thrust or a uniform rate of successive impulses, in Section (II) the author has studied the problem anew according to this mode of propulsion.

When the sounding rocket is ascending through the air the maximum height reached is less than that reached for flight in vacuo. Recently, studies have been made of the problem by W. Ley and H. Schaefer (Ref. 5) and by F. J. Malina and A. M. O. Smith (Ref. 6). On the basis of the latter study a group of new performance parameters have been isolated from the general performance equation, and these are discussed in Section (III).

Notation

Referring to Fig. (4.1), the following notation has been used throughout the paper:

w = weight of propellant and propellant container ejected per impulse, lbs.

k = ratio of container weight to sum of container and propellant weight ejected per impulse.

$\lambda = (1 - k)$

W_0 = initial weight of rocket, lbs.

M_0 = initial mass of the rocket, slugs.

W_p = instantaneous weight of rocket, lbs.

ζ = ratio of initial weight of propellants to initial total weight of a rocket propelled by constant thrust.

ζ_1 = ratio of initial weight of propellants to initial total weight of a rocket propelled by successive impulses.

$\zeta_1' = \zeta_1/\lambda$

n = number of impulses per second.

N = total number of impulses occuring during powered flight.

t = time, sec.

Δt = interval between impulses, sec.

a_0 = initial acceleration imparted to rocket, ft/sec^2.

g_0 = acceleration of gravity at the starting point of flight, ft/sec^2.

g = acceleration of gravity above the starting point of flight, ft/sec^2.

c = effective exhaust velocity of ejected propellant, ft/sec.

v = instantaneous velocity, ft/sec.

Δv_n = velocity imparted to rocket by the n th impulse, ft/sec.

v_n' = velocity at the end of the nth interval, ft/sec.

v_{s_0} = velocity of sound corresponding to the atmospheric conditions at the starting point of the flight, ft/sec.

v_s = velocity of sound corresponding to the atmospheric conditions at the height reached by the rocket at the time t, ft/sec.

β = Mach's number = v/v_s

V_{max} = velocity of rocket at start of coasting flight, ft/sec.

V_{max_0} = velocity of rocket at start of coasting flight if g is constant and equal to g_0, ft/sec.

h = altitude above sea level, feet.

h_n = height reached at the beginning of the nth interval, feet.

h_n' = height reached at the end of the nth interval, feet.

H_p = height traveled during powered flight, feet.

H_{p_0} = height travelled during powered flight, if g is constant and equal to g_0, feet.

H_c = height travelled during coasting flight, feet.

H_{c_0} = height travelled during coasting flight, if g is constant and equal to g_0, feet.

H_{max} = height travelled during powered flight and coasting flight, feet.

H_{max_0} = height travelled during powered flight and coasting flight, if g is constant and equal to g_0, feet.

R = radius of earth, 2.088×10^8, feet.

D = drag on rocket due to air resistance, lbs.

C_D = drag coefficient of rocket shell.

C_D^* = drag coefficient of rocket shell at the velocity of sound.

Λ = drag-weight factor (discussed in the section on the effect of air resistance).

ρ_0 = mass density of air at the starting point of the flight, slugs per cu. ft.

σ = ratio of air densities at altitude and at the starting point of the flight.

T = absolute temperature of the atmosphere at the height reached by the rocket at the time T, ^oF.

T_0 = absolute temperature of atmosphere at the starting point of flight, ^oF.

A = largest cross-sectional area of rocket shell, sq.ft.

d = largest diameter of rocket shell, ft.

ℓ = length of rocket shell, ft.

Section (I)

An approximate method of calculating the maximum height reached by a rocket propelled by powder was developed by R. H. Goddard (Ref. 1). To simplify the analysis a continuous loss of mass was assumed and the problem was so stated that a minimum mass of propellant necessary to lift one pound of mass at the end of the flight to any desired height was determined. However, if high-powered powder is used, the rate of burning is so rapid that the propulsive action is instantaneous. The rocket is thus acted upon by an impulse rather than by a constant thrust.

In the following analysis, it has, therefore, been assumed that the propulsive force is an impulsive force, i.e., the force acts for such a brief interval of time that the rocket does not change its position during the application of the force, although its velocity and its momentum receive a finite change. If the combustion process of the propulsive unit takes place at constant volume this assumption is justified. Further, a study of interior ballistics of small arms reveals that the period between the ignition of the powder charge and the bullet's arrival at the end of a two-

foot barrel is of the order of 14 ten-thousandths of a second. If the gases are not restrained and their travel through the burning chamber and the nozzle is of much shorter length, as is the case for the rocket motor, even shorter periods of duration of action can be expected.

Assuming that the propulsive force acts as an impulse, then the motion of the rocket can be calculated by Newton's third law, which states that impulses between two bodies are equal and opposite. Hence, equating the momentum of the exhaust gases to the momentum imparted to the rocket, using the quantities defined in the list of notation and referring to Fig. 4.1, the following relation can be written for flight in vacuo

$$\frac{\lambda w}{g_0} c = \frac{W_n}{g_0} \Delta v_n \qquad (4.1)$$

where $\lambda = 1 - k$ and $W_n = W_0 - n w$ (4.2)

Or $$\Delta v_n = \frac{w \lambda c}{W_0 - n w} = \frac{\zeta_1' \lambda c}{N} \left(\frac{1}{1 - n \frac{\zeta_1'}{N}} \right) \qquad (4.3)$$

where $$\zeta_1' = \frac{w N}{W_0} = \frac{\zeta_1}{\lambda}$$

During the interval between impulses, Δt, the velocity is reduced by the action of gravity so that at the end of the $n th$ interval, the velocity of the

rocket will be

$$v_n' = v_n - g_0\Delta t - v_{n-1}' + \Delta v_n - g_0\Delta t \qquad (4.4)$$

Therefore

$$v_n' = \sum_{s=1}^{s=n} \Delta v_s - n g_0 \Delta t \qquad (4.5)$$

Substituting for Δv_s from Eq. (4.4)

$$v_n' = \frac{\zeta_1' \lambda c}{N} \sum_{s=1}^{s=n} \frac{1}{1 - s\left(\frac{\zeta_1'}{N}\right)} - n g_0 \Delta t \qquad (4.6)$$

Or $$v_n' = \frac{\zeta_1' \lambda c}{N} S_1 - n g_0 \Delta t$$

where $$S_1 = \sum_{s=1}^{s=n} \frac{1}{1 - s\left(\frac{\zeta_1'}{N}\right)}$$

The height gained during each interval will be represented by the area under the velocity curve in the interval, or

$$h_n' - h_n = v_n'\Delta t + \frac{1}{2} g_0 (\Delta t)^2 \qquad (4.7)$$

Therefore, at the end of the Nth interval which is the end of the powered flight, the height will be

$$H_{p_0} = \sum_{n=1}^{n=N} v_n' \Delta t + \frac{N}{2} g_0 (\Delta t)^2$$

Substituting for v_n' its value in Eq. (4.6)

$$H_{p_0} = \sum_{n=1}^{n=N} \Delta t \left\{ \frac{\zeta_1' \lambda c}{N} \sum_{s=1}^{s=n} \frac{1}{1 - s\left(\frac{\zeta_1'}{N}\right)} - n g_0 \Delta t \right\} + \frac{N}{2} g_0 (\Delta t)^2$$

$$= \frac{\zeta_1' \lambda c}{N} \Delta t \sum_{n=1}^{n=N} \frac{N+1-n}{1 - n\left(\frac{\zeta_1'}{N}\right)} - g_0 (\Delta t)^2 \sum_{n=1}^{n=N} \left(n - \frac{1}{2}\right)$$

$$= \frac{\zeta_1' \lambda c}{N} \Delta t \, S_2 - \frac{N^2}{2} g_0 (\Delta t)^2 \qquad (4.8)$$

where $$S_2 = \sum_{n=1}^{n=N} \frac{N+1-n}{1 - n\left(\frac{\zeta_1'}{N}\right)}$$

The maximum height reached will be the sum of the height at the end of powered flight and the height travelled during coasting or

$$H_{max_0} = H_{p_0} + H_{c_0} = H_{p_0} + \frac{V_{max_0}^2}{2 g_0} \qquad (4.9)$$

To calculate the maximum height one has first to evaluate the sums S_1 and S_2. Noting that

$$\frac{1}{1-s(\frac{\zeta_1'}{N})} = \int_0^\infty e^{-x\{1-s(\frac{\zeta_1'}{N})\}}\,dx$$

S_1 can be written in the form

$$S_1 = \int_0^\infty e^{-x} \sum_{s=1}^{s=n} (e^{x\frac{\zeta_1'}{N}})^s\,dx$$

$$= \int_0^\infty e^{-x} \frac{e^{x\frac{\zeta_1'}{N}} - e^{(n+1)\frac{\zeta_1'}{N}}}{1 - e^{x\frac{\zeta_1'}{N}}}\,dx$$

Putting $\quad x = \frac{Ny}{\zeta_1'} \quad$ the above integral becomes

$$S_1 = -\frac{N}{\zeta_1'}\int_0^\infty e^{-\frac{Ny}{\zeta_1'}}\left(\frac{1-e^{ny}}{1-e^{-y}}\right)dy$$

$$= \frac{N}{\zeta_1'}\left\{\psi\left(\frac{N}{\zeta_1'}\right) - \psi\left(\frac{N}{\zeta_1'}-n\right)\right\} \qquad (4.10)$$

where $\psi(z) = \frac{d}{dz}\{\log\Gamma(z)\}$, the so-called psi-function (Ref. 7,8).

Similarly, S_2 can be summed as

$$S_2 = \frac{N}{\zeta_1'}\left\{N - \left[\frac{N}{\zeta_1'}-(N+1)\right]\left[\psi\left(\frac{N}{\zeta_1'}\right)-\psi\left(\frac{N}{\zeta_1'}-N\right)\right]\right\} \qquad (4.11)$$

Substituting Eqs. (4.10 and (4.11) into Eqs. (4.6) and (4.8), and then into Eq. (4.9) finally

$$H_{max_0} = \frac{\lambda^2 c^2}{2g_0} \Psi^2 - \frac{\lambda c}{n} \left\{ \left(\frac{N}{\zeta_1'} - 1 \right) \Psi - N \right\} \quad (4.12)$$

where $n = \frac{1}{\Delta t}$ and $\Psi = \psi\left(\frac{N}{\zeta_1'}\right) - \psi\left(\frac{N}{\zeta_1'} - N\right)$

For convenience of calculation in Fig. 4.2 the quantity Ψ is plotted against N for different values of ζ_1'.

It can easily be shown that when N = 1

$$\Psi = \frac{\zeta_1'}{1-\zeta_1'}$$

so that Eq. (4.12) reduces to

$$H_{max_0} = \frac{\lambda^2 c^2}{2g_0} \left(\frac{\zeta_1'}{1-\zeta_1'} \right)^2 \quad (4.12a)$$

Also, as $N \rightarrow \infty$, $\Psi \rightarrow -\log(1-\zeta_1')$ thus Eq. (4.12) reduces to

$$H_{max_0} = \frac{\lambda^2 c^2}{2g_0} \left\{ \left[\log(1-\zeta_1') \right]^2 + \frac{\zeta_1' + \log(1-\zeta_1')}{\frac{a_0}{g_0} + 1} \right\} \quad (4.12b)$$

where $a_0 = \frac{\zeta_1'}{N} n \lambda c - g_0 = \frac{n w \lambda c}{W_0} - g_0$ (4.12c)

The quantity a_0 can be considered as the initial acceleration of the rocket if N $\rightarrow \infty$. It is interesting to notice that Eq. (4.12b) is the equation obtained by Malina and Smith (Ref. 6) for calculating the maximum height of a constant thrust rocket, as expected.

Fig. 4.3 shows the variation of $H_{max_0} g_0 / \lambda^2 c^2$ with $n \lambda c / g_0$ for different valves of ζ_1' and for four valves of N. These curves show that when the total number of impulses, N, becomes larger than 100, the maximum height reached is imperceptibly changed by increasing the number.

At this point it is necessary to discuss the similarity existing between a rocket propelled by successive impulses and a rocket propelled by constant thrust. The former loses not only the mass of the propellant, but also the containers for the individual charges. The difference in effect on the rocket between the propellant and its containers is that the propellant has an effective exhaust velocity, c, while the ejected containers leave the rocket without appreciable velocity. The propulsive action, however, will remain the same if the whole cartridge, that is, the propellant charge and its container, is considered wholly as propellant but leaving the motor at a reduced effective exhaust velocity λc. The rocket propelled by constant thrust loses

only the mass equal to the propellant carried, therefore, it can be said to be equivalent to the "successive impulses" rocket if its effective exhaust velocity and its total mass of propellant are equal respectively to the reduced exhaust velocity and to the sum of the masses of all the containers of the "successive impulses" rocket. In other words, c is equal to λc and ζ is equal to ζ_1'.

In Table 4.1 the heights for four cases have been calculated to illustrate the effect of the exhuast gas velocity and the total number of impulses given to a rocket whose weight ratio, ζ_1' is 0.70. It will be noticed that for flight in vacuo a greater height will be reached if a smaller number of impulses is employed. The lower portion of the Table shows the maximum height reached by an equivalent "constant thrust" rocket for the same four cases with the initial acceleration given by Eq. (4.12c). The close agreement between the maximum height reached by use of successive impulses, when the total number of impulses exceeds 100, and that reached by the use of constant thrust simplifies the solution of the problem of decreasing acceleration of gravity with height, and enables prediction for flight with air resistance to be based on the results obtained for a rocket propelled by constant thrust (c.f. Ref. 6). These problems are considered in the following sections.

Section (II)

It is well-known that the acceleration of gravity decreases with the height above the earth's surface according

TABLE 4.1

Successive impulses

$$H_{max_0} = \frac{\lambda^2 c^2}{g_0}\left\{\frac{1}{2}\Psi^2 - \frac{1}{\frac{n\lambda c}{g_0}}\left[\left(\frac{N}{\zeta_1'} - 1\right)\Psi - N\right]\right\}$$

Case	Ft./sec. λc	ζ_1'	N	n Impulses per sec.	H_{max_0} Feet
1	10,000	0.70	326	3	1,472,000
2	10,000	0.70	10	0.092	1,686,000
3	7,000	0.70	326	3	560,000
4	7,000	0.70	10	0.092	676,000

Constant Thrust

$$H_{max_0} = \frac{c^2}{g_0}\left\{\frac{1}{2}\left[\log(1-\zeta)\right]^2 + \frac{1}{\frac{a_0}{g_0}+1}\left[\log(1-\zeta)+\zeta\right]\right\}$$

Case	Ft./sec. c	ζ	a_0	H_{max_0} Feet
1	10,000	0.70	32.2	1,468,000
2	10,000	0.70	32.2	1,468,000
3	7,000	0.70	12.9	555,000
4	7,000	0.70	12.9	555,000

to the following relation

$$g = g_o \left(\frac{R}{R+h}\right)^2 \qquad (4.13)$$

At an altitude of 1000 miles the acceleration is only 0.64 times that at sea level. Therefore, for flights up to such altitudes the assumption that g is approximately constant is no longer valid. It was shown by Malina and Smith (Ref. 6) that a three-step rocket could theoretically reach such an altitude. Thus it is interesting to see how the decrease of g will increase the maximum height reached by the rocket.

First the effect on powered flight in vacuo will be considered and then on coasting flight in vacuo. For powered flight the analysis is based on the assumption that the thrust is constant. However, the results can be applied to the case of propulsion by successive impulses if the total number of impulses, N, exceeds 100 as was justified in the previous section.

The equivalent mass of gas flowing per second continuously for the case of successive impulses is

$$\frac{wn}{g_o} = m \qquad (4.14)$$

Assuming that the rocket starts from rest at sea level the equation of motion in vacuo is

$$\frac{d^2h}{dt^2} = -g_0 \left(1 + \frac{h}{R}\right)^{-2} + \frac{\frac{mc}{M_0}}{1 \quad \frac{m}{M_0} t} \tag{4.15}$$

This is a non-linear differential equation which can not be solved by usual means. However, for all practical purposes the ratio $\frac{h}{R}$ during powered flight is much smaller than 1, therefore, only first order terms in $\frac{h}{R}$ occurring in the expansions need to be retained. This approximation linearizes the equation to the form

$$\frac{d^2h}{dt^2} = g_0 \left(\frac{2h}{R} - 1\right) + \frac{\frac{mc}{M_0}}{1 - \frac{m}{M_0} t} \tag{4.16}$$

The solution of this equation with the initial condition that $h = 0$ and $\frac{dh}{dt} = 0$ when $t = 0$ is

$$h = \frac{R}{2}\left\{1 - \cosh\sqrt{\frac{2g_0}{R}}\, t\right\} + \frac{C}{2\sqrt{\frac{2g_0}{R}}}\left\{e^{\xi u}\int_{\xi}^{\xi u} \frac{e^{-x}dx}{x} - e^{-\xi u}\int_{\xi}^{\xi u} \frac{e^{x}dx}{x}\right\} \tag{4.17}$$

where $\xi = \sqrt{\frac{2g_0}{R}}\frac{M_0}{m}$. and $u = 1 - \frac{m}{M_0} t$

At the end of the powered flight, the time is

$$t = t_p = \frac{M_0 \xi}{m} \tag{4.18}$$

Therefore, the height at the end of the powered flight is

$$H_p = \frac{R}{2}\left\{1 - \cosh\sqrt{\frac{2g_0}{R}\frac{M_0\zeta}{m}}\right\} + \frac{c}{2}\sqrt{\frac{R}{2g_0}}\left\{e^{\xi(1-\zeta)}\int_{\xi}^{\xi(1-\zeta)}\frac{e^{-x}dx}{x} - e^{-\xi(1-\zeta)}\int_{\xi}^{\xi(1-\zeta)}\frac{e^{x}dx}{x}\right\} \quad (4.19)$$

If the hyperbolic cosine term and the integrals are expanded and only first order terms in $\frac{1}{R}$ are retained in consistency with the linearization of Eq. (4.15), the equation becomes

$$H_p = -\left\{\frac{\zeta^2 g_0}{2}\left(\frac{W_0}{w}\right)^2 + \frac{\zeta^4 g_0^2}{12R}\left(\frac{W_0}{w}\right)^4\right\} + c\frac{W_0}{w}\left\{(1-\zeta)\log(1-\zeta)+\zeta\right\}$$

$$+ \frac{cg_0}{18R}\left(\frac{W_0}{w}\right)^3\left\{6(1-\zeta)^3\log(1-\zeta)+\zeta(11\zeta^2-15\zeta+6)\right\} \quad (4.20)$$

$$= H_{p_0} + \frac{g_0}{6R}\left(\frac{W_0}{w}\right)^3\left\{\frac{c}{3}\left[6(1-\zeta)^3\log(1-\zeta)+\zeta(11\zeta^2-15\zeta+6)\right] - \frac{\zeta^4 g_0}{2}\left(\frac{W_0}{w}\right)\right\}$$

Differentiating Eq. (4.17), and substituting the relation of Eq. (4.18), the maximum velocity at the end of powered flight is

$$V_{max} = -\sqrt{\frac{Rg_0}{2}}\sinh\sqrt{\frac{2g_0}{R}\frac{M_0\zeta}{m}} - \frac{c}{2}\left\{e^{\xi(1-\zeta)}\int_{\xi}^{\xi(1-\zeta)}\frac{e^{-x}dx}{x} - e^{-\xi(1-\zeta)}\int_{\xi}^{\xi(1-\zeta)}\frac{e^{x}dx}{x}\right\} \quad (4.21)$$

Again expanding and retaining only first order terms in $\frac{1}{R}$, Eq. (4.21) becomes

$$V_{max} = -\left\{\left(\frac{W_0}{w}\right)\zeta + \frac{1}{3}\frac{\zeta^3 g_0^2}{R}\left(\frac{W_0}{w}\right)^3\right\} -$$

$$-\left\{c \log(1-\zeta) + \frac{c g_0}{2R}\left(\frac{W_0}{w}\right)^2\left[2(1-\zeta)^2\log(1-\zeta) + 2\zeta - 3\zeta^2\right]\right\}$$

$$= V_{max_0} - \frac{g_0\left(\frac{W_0}{w}\right)^2}{R}\left\{\frac{\zeta^3 g_0\left(\frac{W_0}{w}\right)}{3} + \frac{c}{2}\left[2(1-\zeta)^2\log(1-\zeta) + 2\zeta - 3\zeta^2\right]\right\} \tag{4.22}$$

It is seen that the second terms of Eq. (4.20) and (4.22) are the correction to be applied to H_{p_0} and V_{max_0} to account for the variation of the acceleration of gravity. Since both corrections are first order approximations, they can be expected to apply approximately also to the case of successive impulses, even when the total number of impulses is less than 100.

The coasting height reached by the rocket due to its velocity at the end of powered flight can be obtained by equating the increase of potential energy during coasting flight to the kinetic energy at the end of powered flight. Thus

$$\frac{1}{2} V_{max}^2 = g_0 \int_{H_p}^{H_p+H_c} \frac{dh}{\left(1+\frac{h}{R}\right)^2}$$

or

$$H_c = (H_p + R)\left\{ \frac{1}{1 - \frac{V_{max}^2}{2g_0\left(\frac{R}{H_p+R}\right)^2 (H_p+R)}} - 1 \right\} \tag{4.23}$$

Putting $V_{max}^2 / 2g_0 \left(\frac{R}{R+H_p}\right)^2 = H_{c_0}$ which is coasting height obtained by assuming a constant gravitational acceleration of the value equal to that at the height H_c i.e., the height where coasting starts, then Eq. (4.23) can be written

$$H_c = (H_p + R)\left\{ \frac{1}{1 - \frac{H_{c_0}}{H_p+R}} - 1 \right\}$$

Upon expanding the second term this equation becomes,

$$H_c = H_{c_0}\left\{ 1 + \left(\frac{H_{c_0}}{H_p+R}\right) + \left(\frac{H_{c_0}}{H_p+R}\right)^2 + \left(\frac{H_{c_0}}{H_p+R}\right)^3 + \cdots \right\} \tag{4.24}$$

This equation shows that if the coasting flight starts from sea level, and if the maximum height reached is about 1000 miles, the increase due to the decrease in g is over 25%, which is considerable.

Section (III)

When the sounding rocket is ascending through the atmosphere instead of in vacuo, air resistance comes into play, causing the acceleration of the rocket to be reduced, which decreases the maximum height reached. Since air resistance increases with the air density and with the square of the flight velocity, it is desirable to keep the rocket from ascending too rapidly through the lower layers of the atmosphere where the air density is high. For this reason the optimum initial acceleration will no longer be infinite as shown by Eq. (4.12b). For the case of constant thrust Malina and Smith (Ref. 6) have found that the optimum acceleration is around 30ft./sec.^{2}. For a total number of impulses greater than 100, the difference between propulsion by successive impulses and by constant thrust is very small, so one may expect the above optimum value of initial acceleration to hold for both cases of propulsion.

The actual amount of reduction in maximum height due to air resistance can be calculated by the method of step-by-step integration, if fair accuracy is desired. This integration is carried out by using the fundamental equation for vertical rocket flight which, as given in the previous paper (Ref.6) is

$$\frac{d^2h}{dt^2} = a = -g + \frac{a_0 + g_0}{1 - \frac{t(a_0+g_0)}{c}} - \frac{g_0 \rho_0 \sigma v^2}{2\left[1 - \frac{t(a_0+g_0)}{c}\right]} \frac{C_D A}{W_0} \qquad (4.25)$$

The significance of the ratio $\frac{C_D A}{W_0}$ was discussed in that paper (Ref. 6). Greater significance can, however, be attached to the various terms in the equation if it is transformed into the non-dimensional form

$$\frac{a}{g_0} = -\frac{g}{g_0} + \frac{\frac{a_0}{g_0}+1}{1-\frac{g_0 t}{c}\left(\frac{a_0}{g_0}+1\right)} - \frac{\left(\sigma\frac{T}{T_0}\right)\left(\frac{C_D}{C_D^*}B^2\right)\Lambda}{1-\frac{g_0 t}{c}\left(\frac{a_0}{g_0}+1\right)} \qquad (4.26)$$

$$\text{where} \quad \Lambda = \frac{\frac{\rho_0}{2} C_D^* A v_{s_0}^2}{W_0}$$

In Eq. (4.26) appear two types of significant quantities. First, quantities, called "factors", which are constant for any given family of rockets, and second, two quantities called "parameters", one of which is characteristic for a given family of rockets but changes in value along the flight path, and one which depends on the physical properties of the atmosphere. Thus there are the following factors:

$\frac{a_0}{g_0}$ = ratio of initial acceleration to g_0 "initial acceleration factor", a motor characteristic

c = exhaust velocity in ft./sec. $\sim$ "exhaust velocity factor", a motot characteristic

Λ = "drag-weight factor"

ζ = ratio of weight of combustibles to total initial weight of the rocket $\sim$ "loading factor"

The first two factors, i.e., the "initial acceleration factor" and the "exhuast velocity factor", determine the characteristics of the propelling unit for a given family of rockets while the "drag-weight factor" and the "loading factor" determine the physical dimensions of the rockets. The "drag-weight factor" is a ratio of the drag of the rocket at sea level when traveling with the velocity of sound to the initial weight of the rocket. Since for any given family of rocket shapes the only terms in the factor which can be varied are the maximum cross-sectional area A, and the initial weight W_o, it is clear that if the initial weight is doubled then the cross-sectional area must also be doubled to keep the factor the same. The "loading factor needs to be discussed in some detail as it does not appear explicitly in Eq. (4.26). The Eq.(4.26) is a differential equation of the flight path which is satisfied at every point along the flight path. The loading factor ζ comes in only when this equation is integrated and the limits of integration are put in. For example, consider two rockets with identical performance factors and parameters, with the exception that one has a ζ of 0.90 and the other has a ζ of 0.50. The flight path of the two rockets will be

identical up to the time that 0.50 times the initial weight of the rockets is used up as combustibles. At this point the rocket having a ζ of 0.50 will begin to decelerate while the one having a ζ of 0.90 will continue to accelerate until the remaining combustibles are used up. It is thus seen that the value of ζ controls the maximum height reached.

The two performance parameters are:

$\sigma \frac{T}{T_0}$ ~ physical properties of the atmosphere called the "atmosphere parameter"

$\frac{C_D}{C_D^*}$ ~ aerodynamic properties of the rocket shell called the "form parameter"

The "atmosphere parameter" for the earth's atmospheric layer will, of course, be the same for all rockets if standard conditions are assumed and its value depends only on the height the rocket has reached above the starting point of the flight. The "form parameter" is determined by the shape of the curve of C_D against B. This curve will be altered chiefly by the geometrical shape of the shell although it is also affected by the change in skin friction coefficient due to the change in Reynold's Number. As long as the rocket belongs to a family that has the same geometrical shape, which implies the same nose shape and the same l/d ratio, that is, the ratio of the length of the shell to the maximum diameter, the "form parameter" can be assumed to remain constant.

It is thus seen that the performance curves calculated for a typical rocket will also hold for a whole family of rockets determined by the values of the "factors" and of the "parameters" of the typical rocket and the design of a rocket to meet certain prescribed requirements is greatly simplified. Furthermore, for a good rocket form design the variation of $\frac{C_D}{C_D^*} B^2$, the form parameter, at the same values of B is small. Also, the deviation from standard atmospheric characteristics cannot be very large. Then, in view of the fairly accurate but not exact basic assumption of constant thrust, it is justified to use the same data for these two parameters for all cases. Thus, the performance problem is further simplified and depends only upon the four performance factors $\frac{a_0}{g_0}$, c , Λ and ζ .

CONCLUSION

This study shows that a sounding rocket propelled by successive impulses can theoretically reach heights of much use to thoseinterested in obtaining data on the structure of the atmosphere and extra-terrestial phenomena if a propelling unit gives an exhaust velocity of 7000 ft. per second or more.

The possibility of obtaining such exhaust velocities depends on two factors: first, the ability of the motor to transform efficiently the heat energy of the fuel into kinetic energy of the exhaust gases, and secondly, the amount of heat energy that can be liberated from the fuel. In an actual motor which burns its fuel at constant volume by igniting a powder charge in the combustion chamber the ratio of the chamber pressure to the outlet pressure drops from a maximum at the beginning of the expansion to zero at the end of the process. It is not possible to design a nozzle that will expand the products of combustion smoothly during the whole process. Therefore, the attainable efficiency must be less than that of a corresponding "constant pressure" motor which has a mixture of combustibles, e.g. gasoline and liquid oxygen, fed continuously into the combustion chamber at a constant pressure equal to the maximum pressure of the "constant volume" motor. However, very high maximum chamber pressures (up to 60,000 lbs.

per sq.in.) can be developed in a motor using constant volume burning, while the chamber pressure of a motor using constant pressure burning is limited to much lower pressures by the difficulty of feeding the combustibles. Therefore, the efficiency that can be obtained frommotors using either of these processes should not be very different. As to the heat that can be liberated per unit mass of fuel, the present fuel, such as nitro-cellulose powder for a constant volume motor, is much lower than the liquid combustibles such as gasoline and oxygen for a constant pressure motor.

These considerations indicate that the attainable exhaust velocity of a "constant volume" motor for propulsion by successive impulses will probably be lower than that of a "constant pressure" motor for supplying a continuous thrust. This is the reason why many experimenters abandoned the "constant volume" motor and turned to the "constant pressure" motor, the so-called liquid propellant motor. Theoretically, this defect of the "constant volume" motor can be compensated if a small total number of impulses (c.f. Fig. 4.3) is used. However, the use of few impulses is of doubtful practical value because the resulting extreme accelerations will be harmful to instruments carried and will necessitate a heavier construction of the rocket.

However, even with the lower exhaust velocities of the "constant volume" motor it is shown by the analysis in this paper that with the exhaust velocity of 7000 ft./sec. obtained experimentally by R. H. Goddard (Ref. 1) it should be possible to build a poder rocket capable of rising above 100,000 feet. Thus it seems to the author that a rocket propelled by successive impulses has useful possibilities and further experimental work is justified.

REFERENCES ON PART (IV)

1. Goddard, R. H.: "A Method of Reaching Extreme Altitudes", Smithsonian Miscellaneous Collections, Vol.71, No. 2, 1919.

2. Damblanc, L. : "Les fusées autopropulsives à explosifs", L'Aérophile, Vol. 43 pp.205-209 and pp. 241,-247, 1935.

3. Bartocci, A.: "Le éscursioni in altezza col motore a reazione", L'Aerotecnica, Vol 13, pp. 1646-1666, 1933.

4. Breguet, L. and Devillers, R. : "L'Aviation superatmosphérique, les aérodynes propulsées par reaction directe", La Science Aérienne, Vol. 5, pp. 183-222, 1936.

5. Ley, W. and Schaefer, H.: "Les fusées volantes météorologiques", L'Aérophile, Vol. 44, pp.228-232, 1936.

6. Malina, F. J. and Smith, A.M.O. : "Analysis of the Sounding Rocket", Jour. of Aero. Sciences, Vol. 5, pp. 199-202, 1938.

7. Whittaker and Watson: "Modern Analysis", pp. 246-247, 4th Edition, 1927, Cambridge.

8. Davis, H. T. :"Tables of the Higher Mathematical Functions", Vol. 1, pp. 277-364, 1st Edition, 1933, Principia Press.

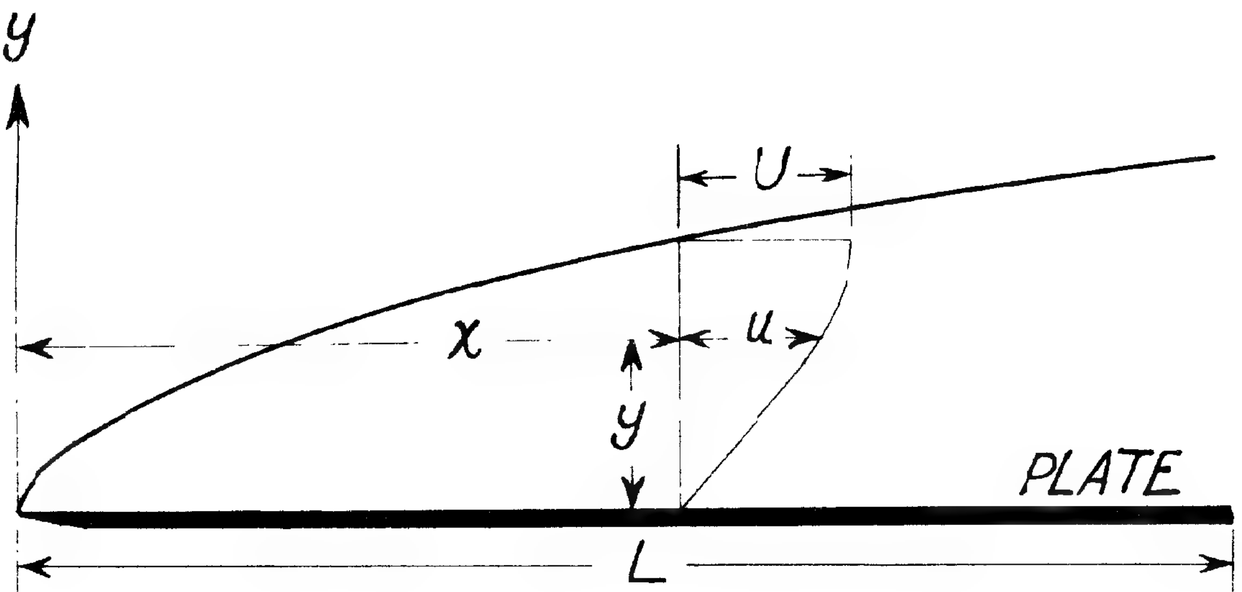


Fig. 1.1

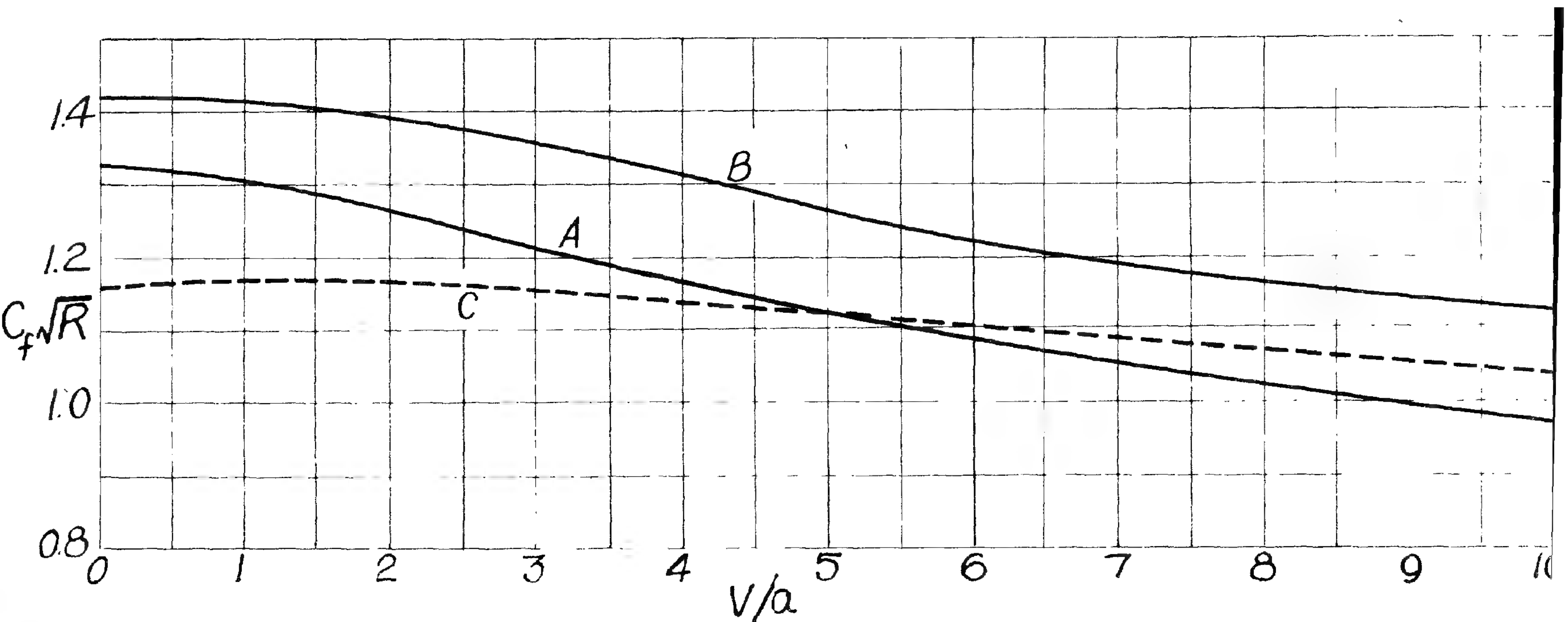


Fig. 1.2 Skin friction coefficients. (a) No heat transferred to wall
(b) Wall temperature 1/4 of free stream temperature
(c) von Karman's first approximation

Fig. 1.3 Velocity and temperature distribution when no heat is transferred to wall

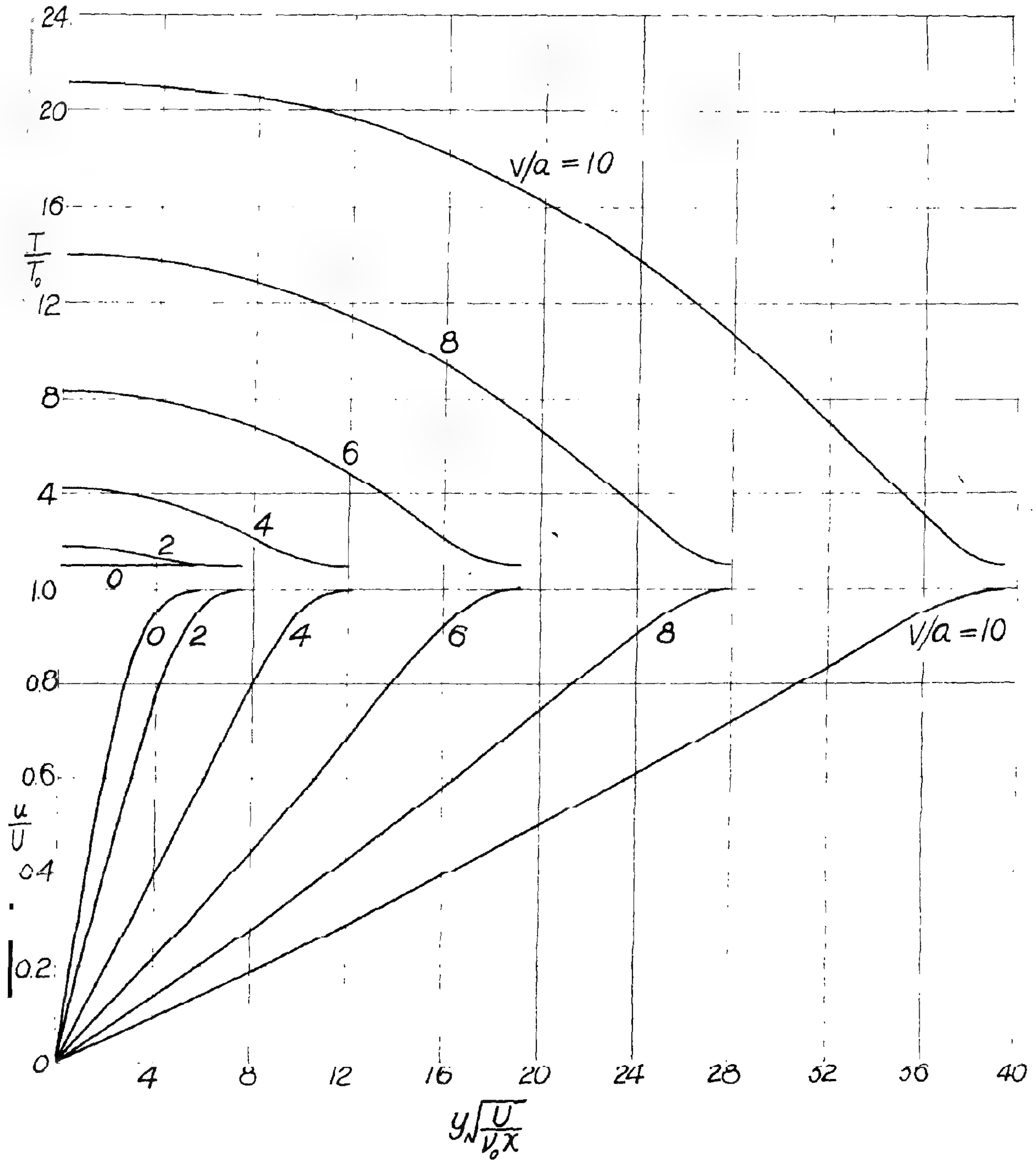
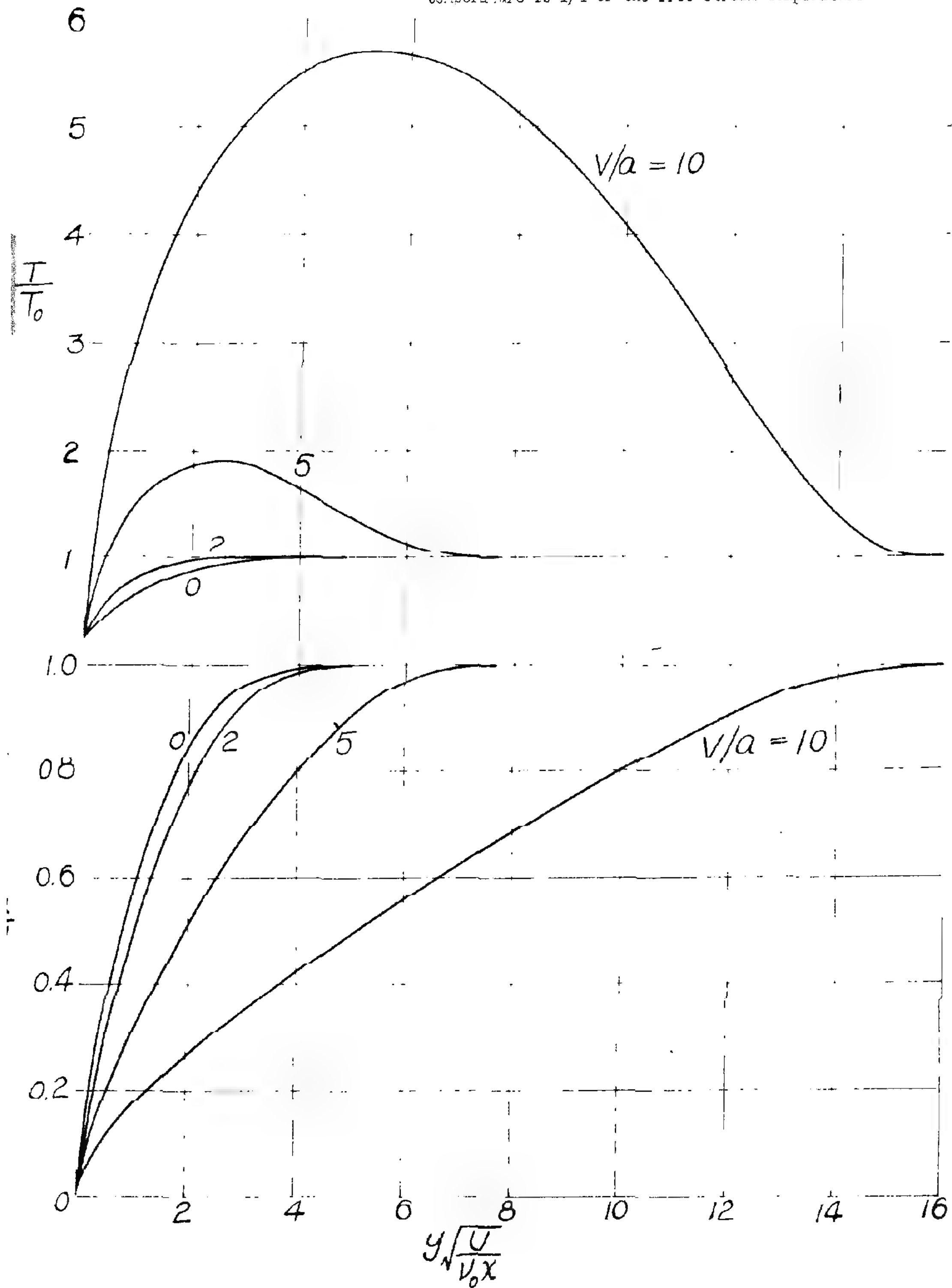


Fig. 1.4 Velocity and temperature distribution when wall temperature is 1/4 of the free stream temperature



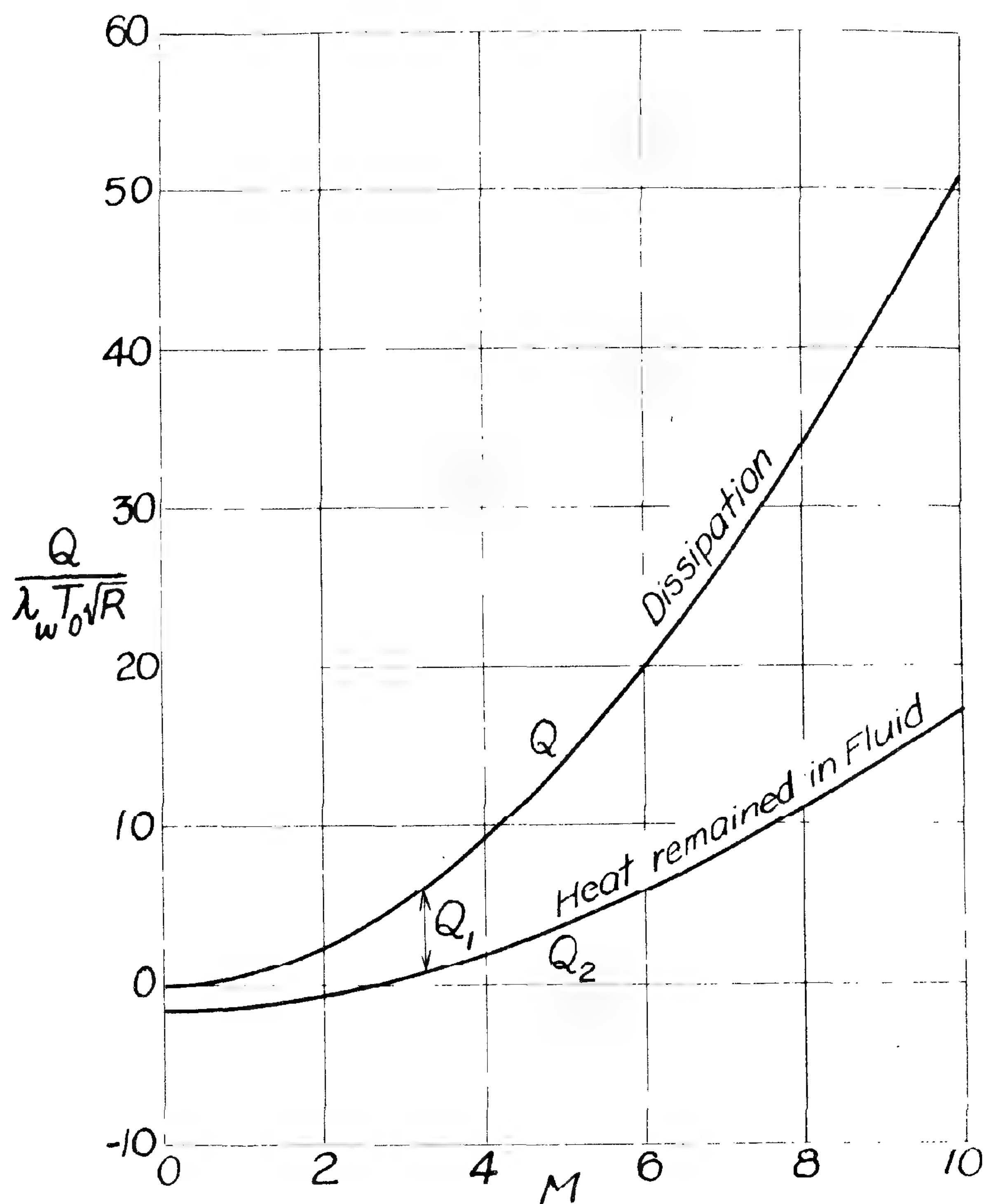


Fig. 1.5 Heat balance when the wall temperature is 1/4 of the free stream temperature

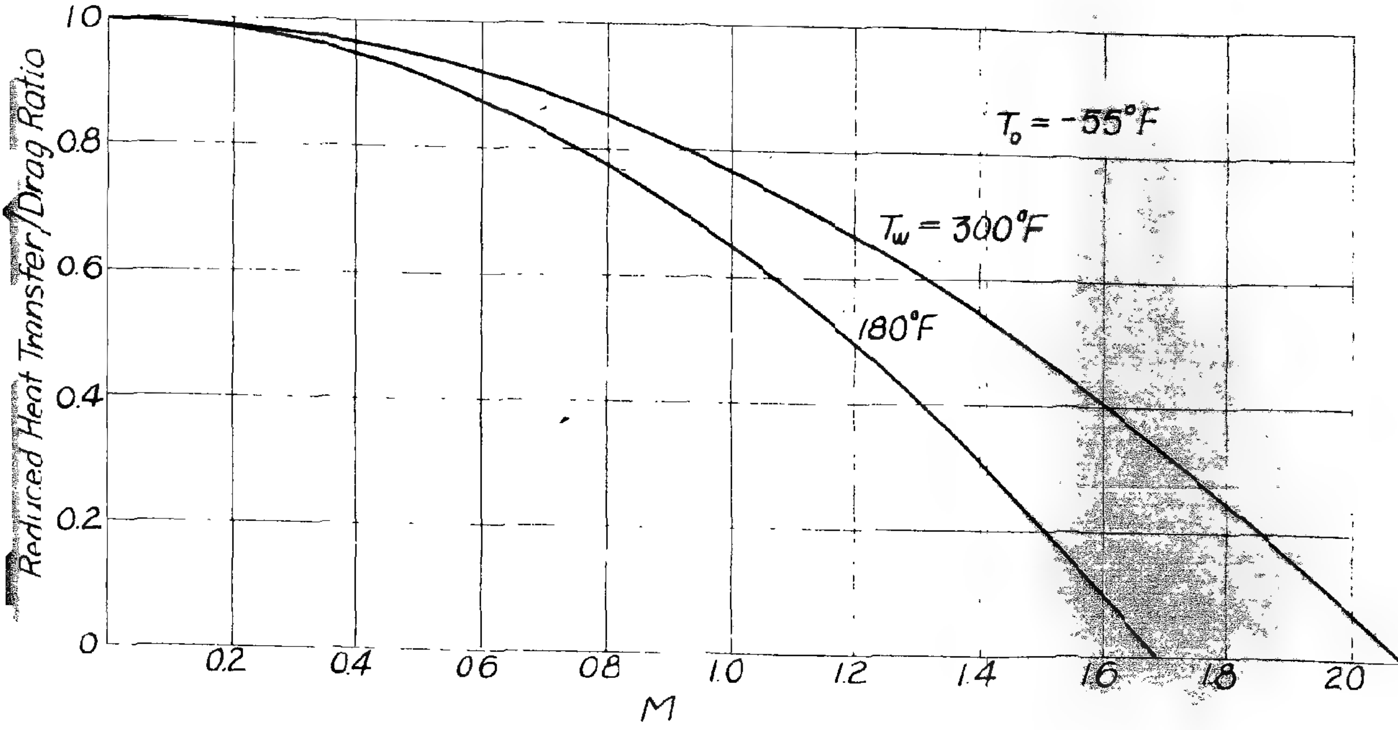


Fig. 1.6 The effect of high speed on cooling efficiency

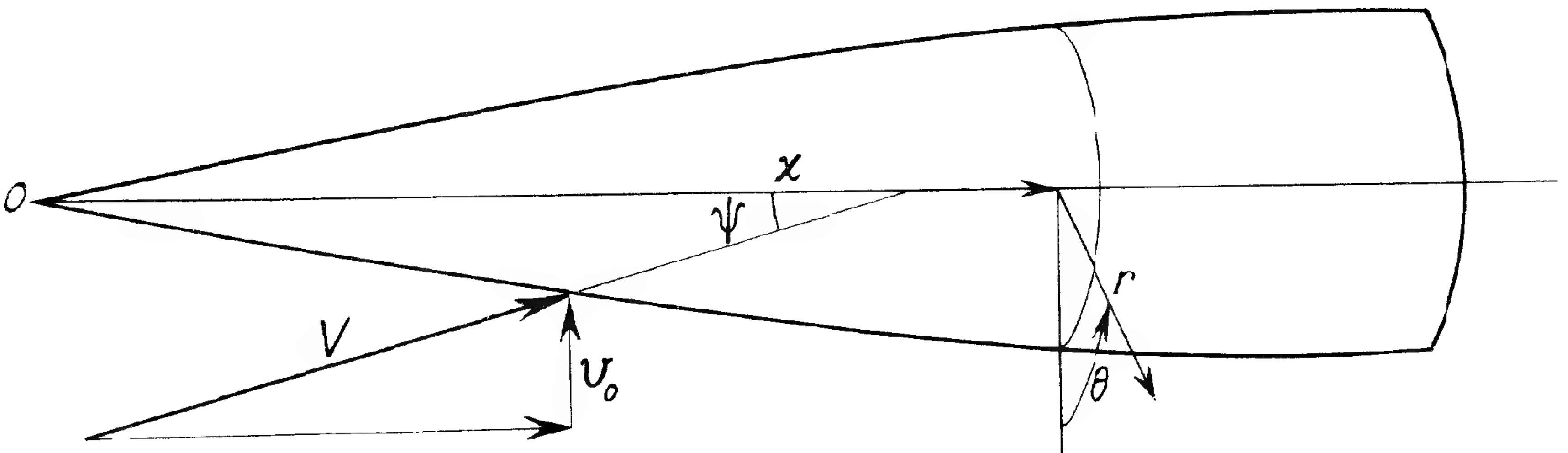


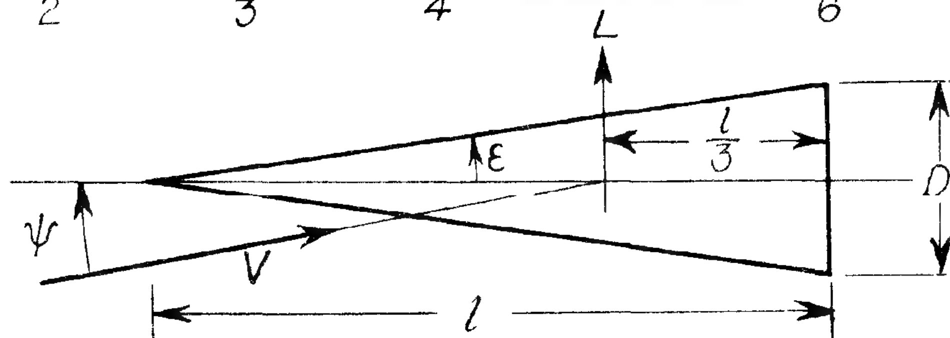
Fig. 2.1

$\frac{dC_L}{d\psi}$

2.0
1.8
1.6
1.4
1.2
1.0

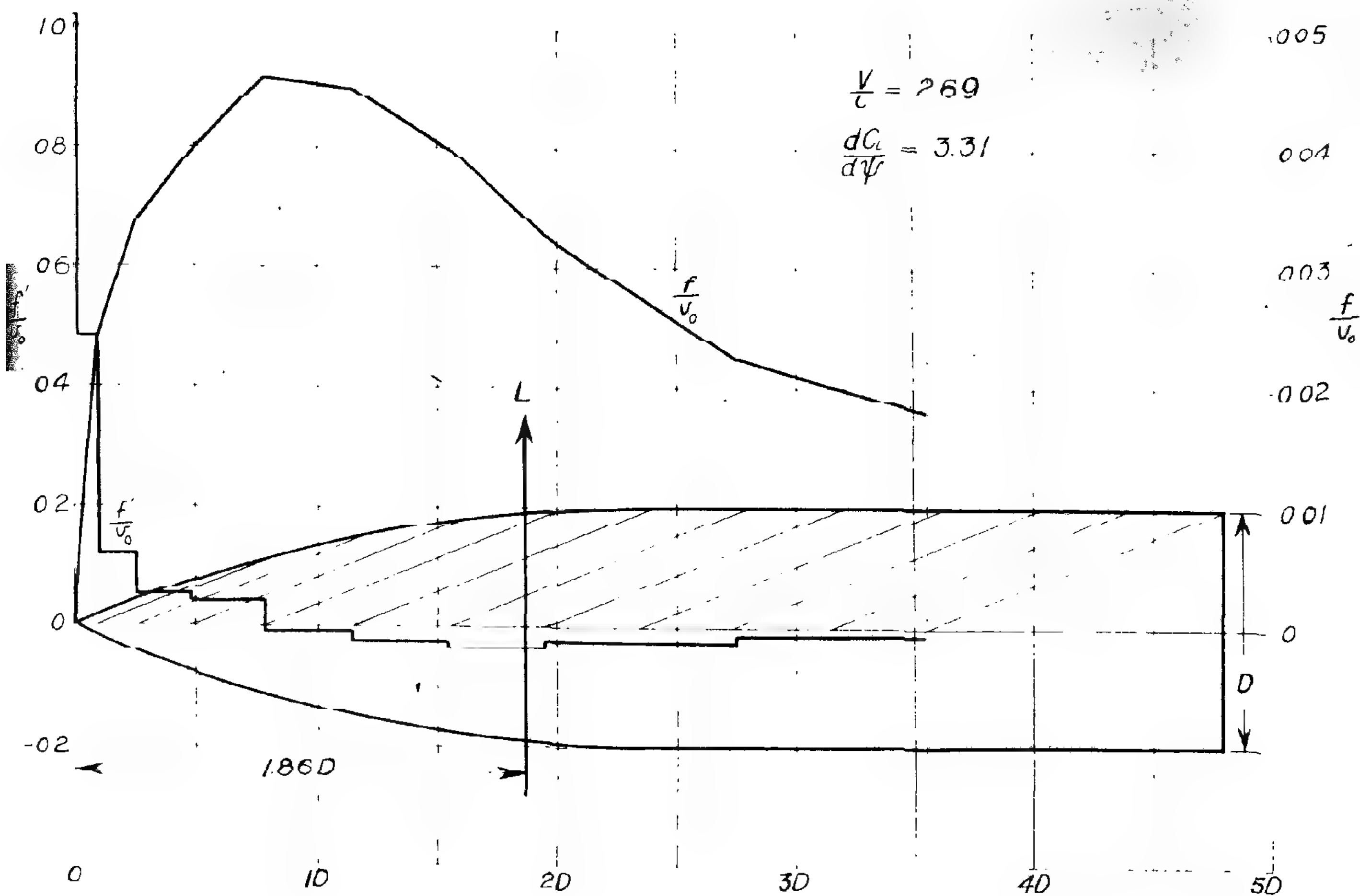
1 2 3 4 5 6 7 8 $\frac{V}{c}$

$\varepsilon - 5°$
10°
15°
20°
25°



$$C_L = \frac{L}{(\rho/2)\frac{\pi D^2}{4}}$$

Fig. 2.2



1.0
.08
.06
.04
.02
0
-.02
.005
.004
.003
.002
.001
0
$\frac{V}{c} = 269$
$\frac{dC_L}{d\psi} = 3.31$
$\frac{f}{V_0}$
$\frac{f'}{V_0}$
L
D
1.86D
0
1D
2D
3D
4D
5D

Fig. 2.3

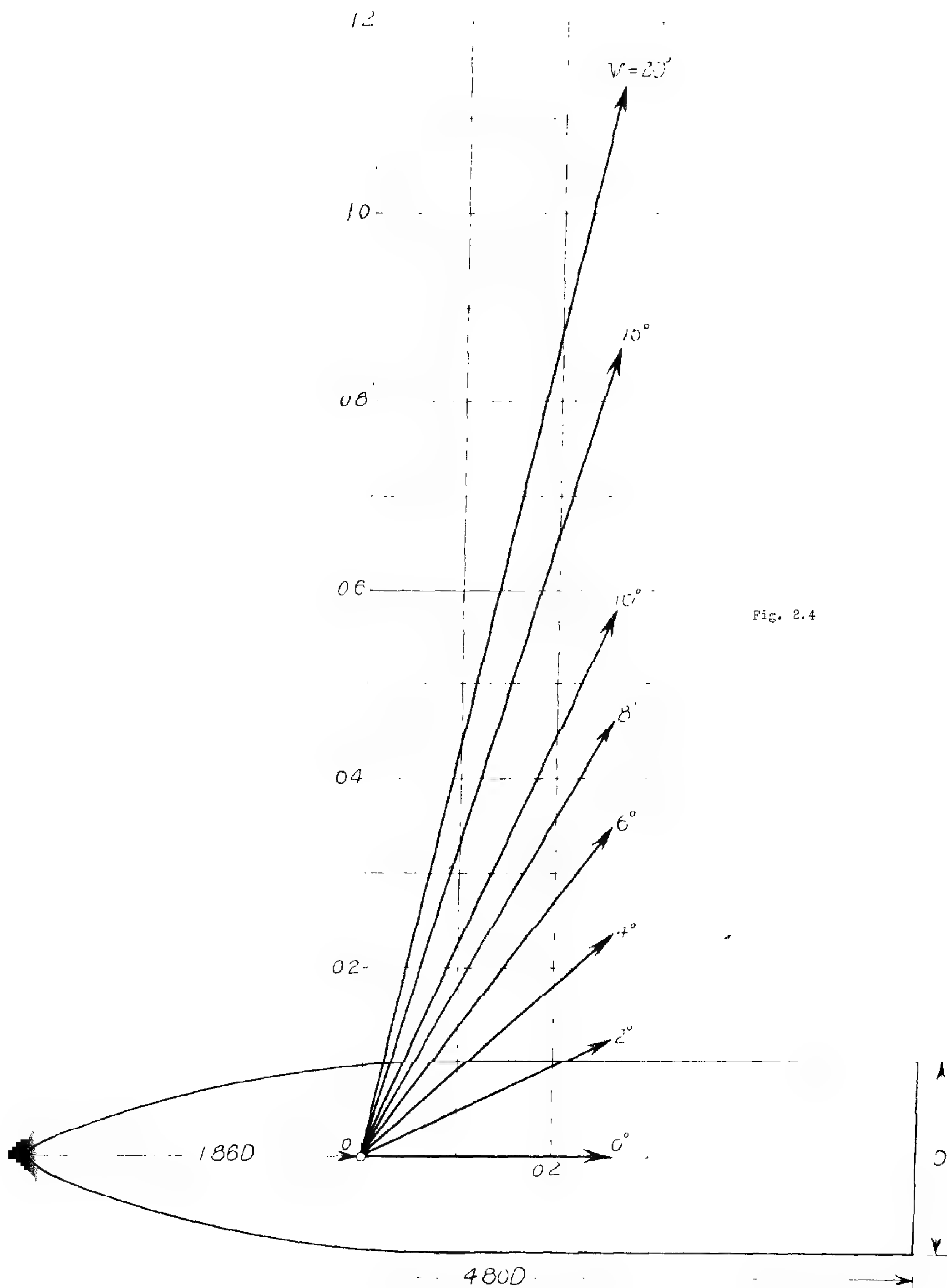


Fig. 2.4

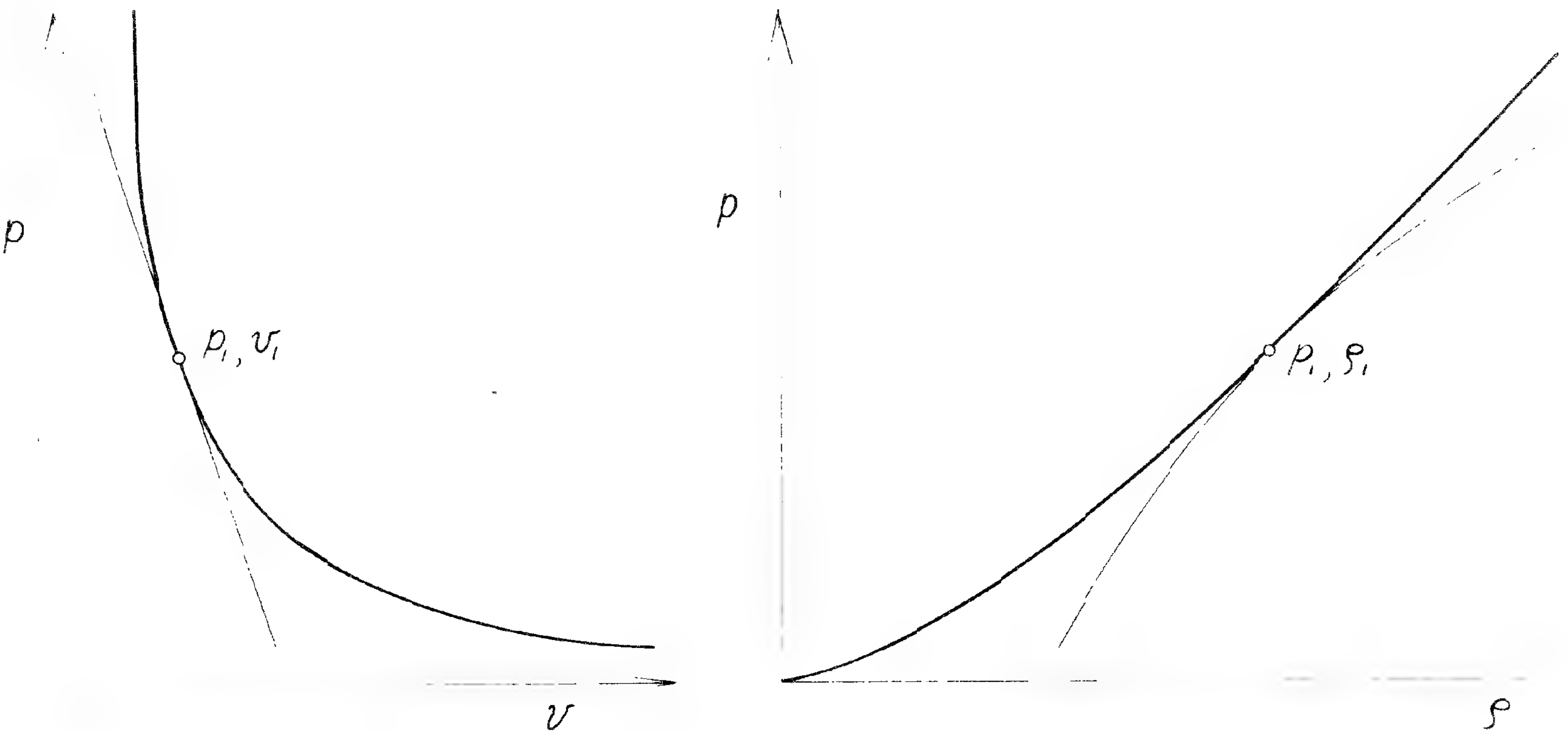


Fig. 3.1 The approximation of adiabatic curve by its tangent

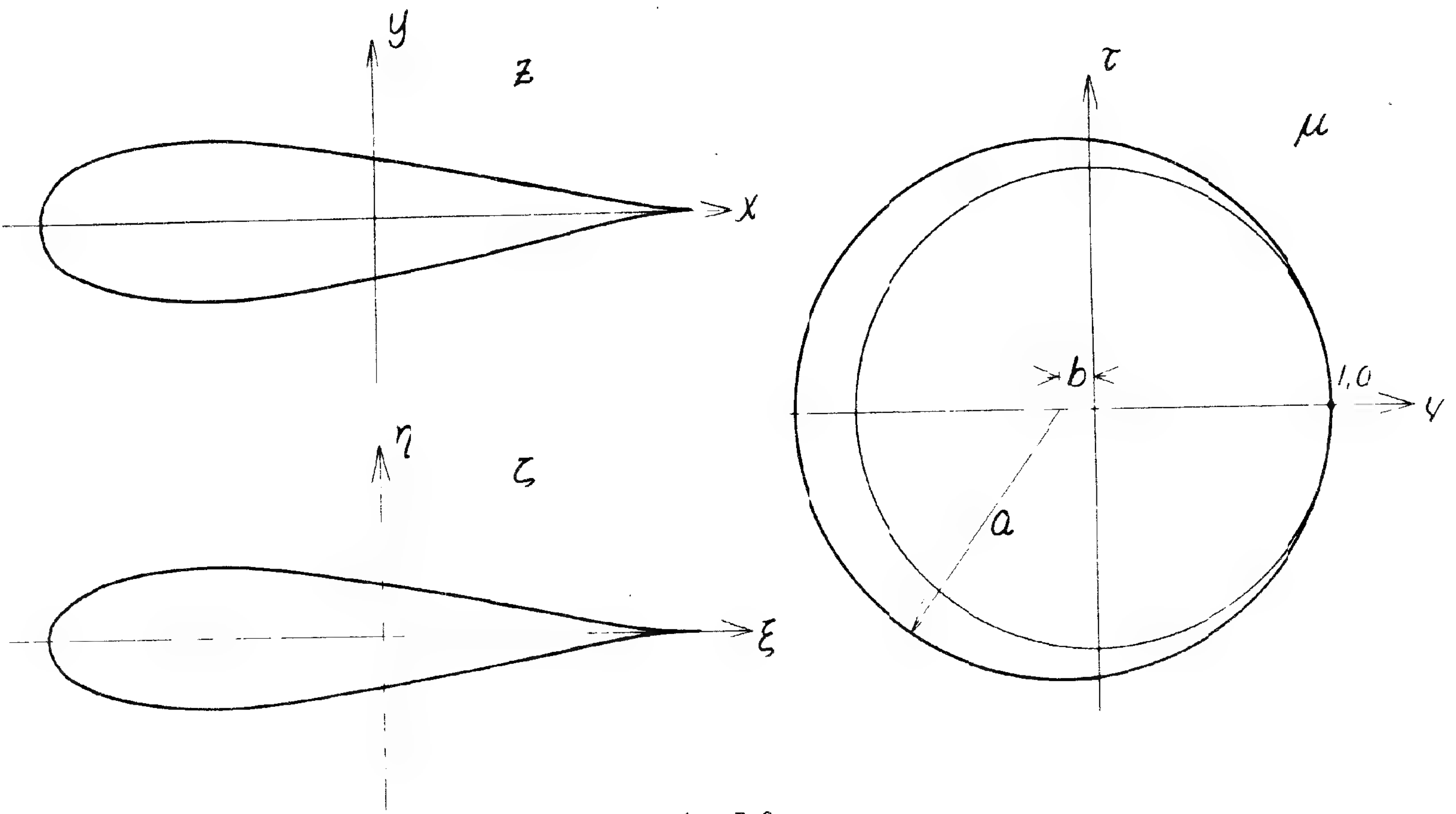
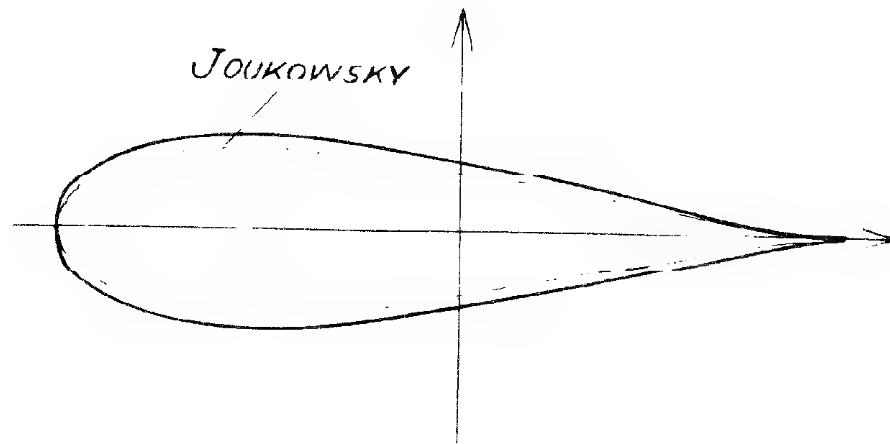
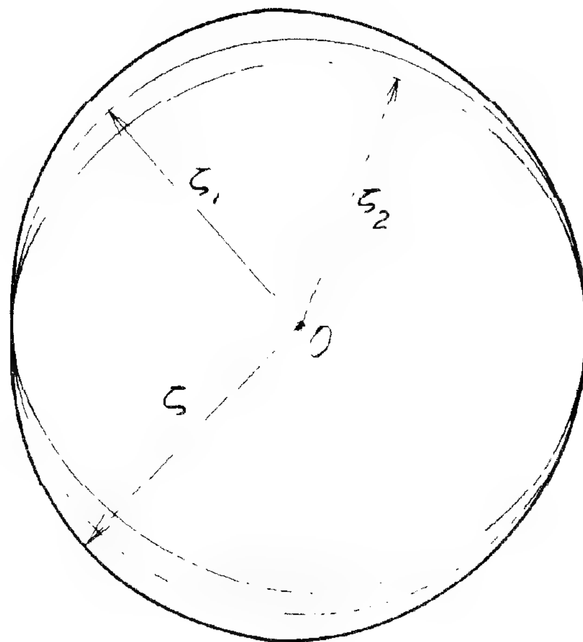


Fig. 3.2

Fig. 3.4





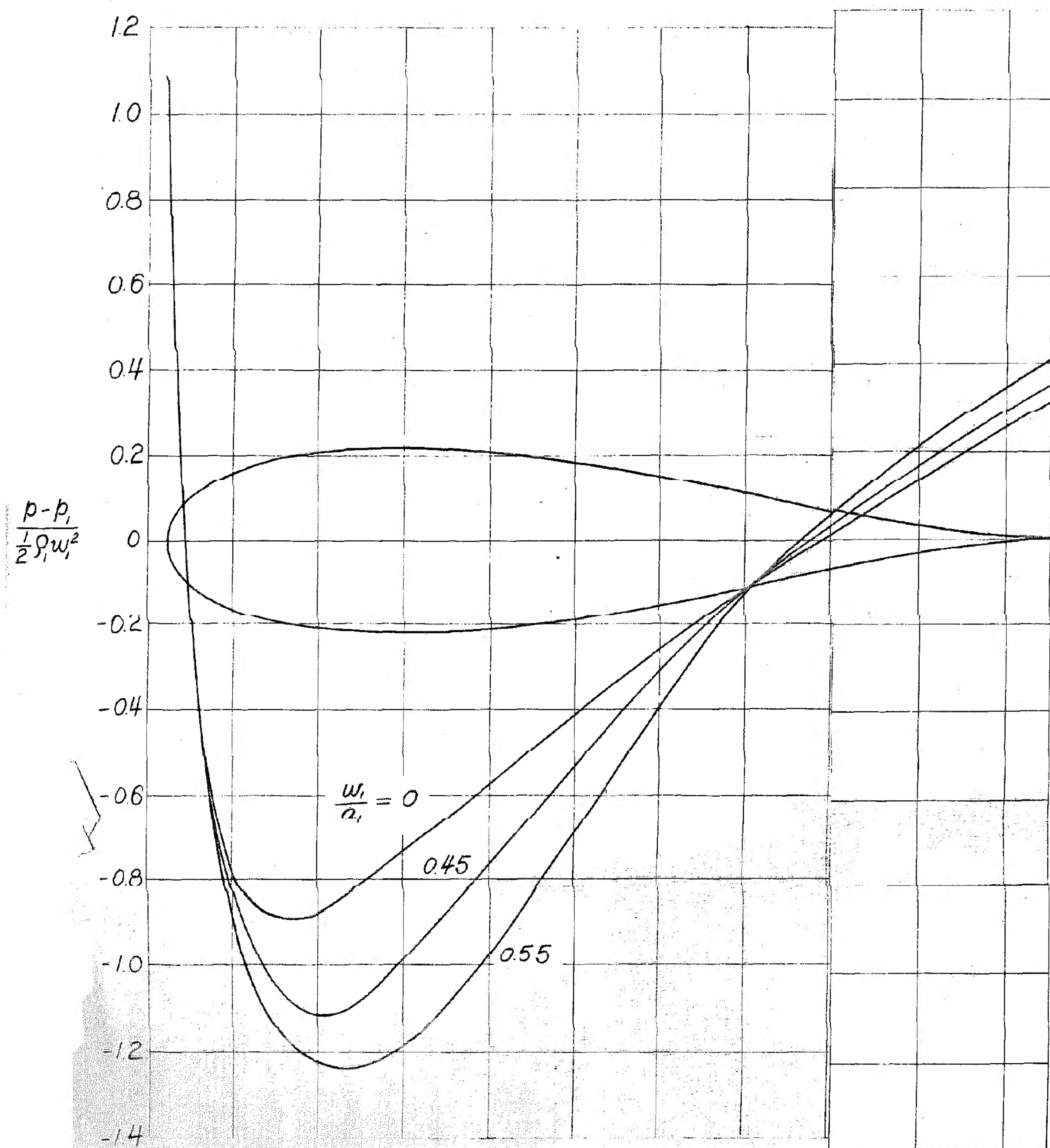
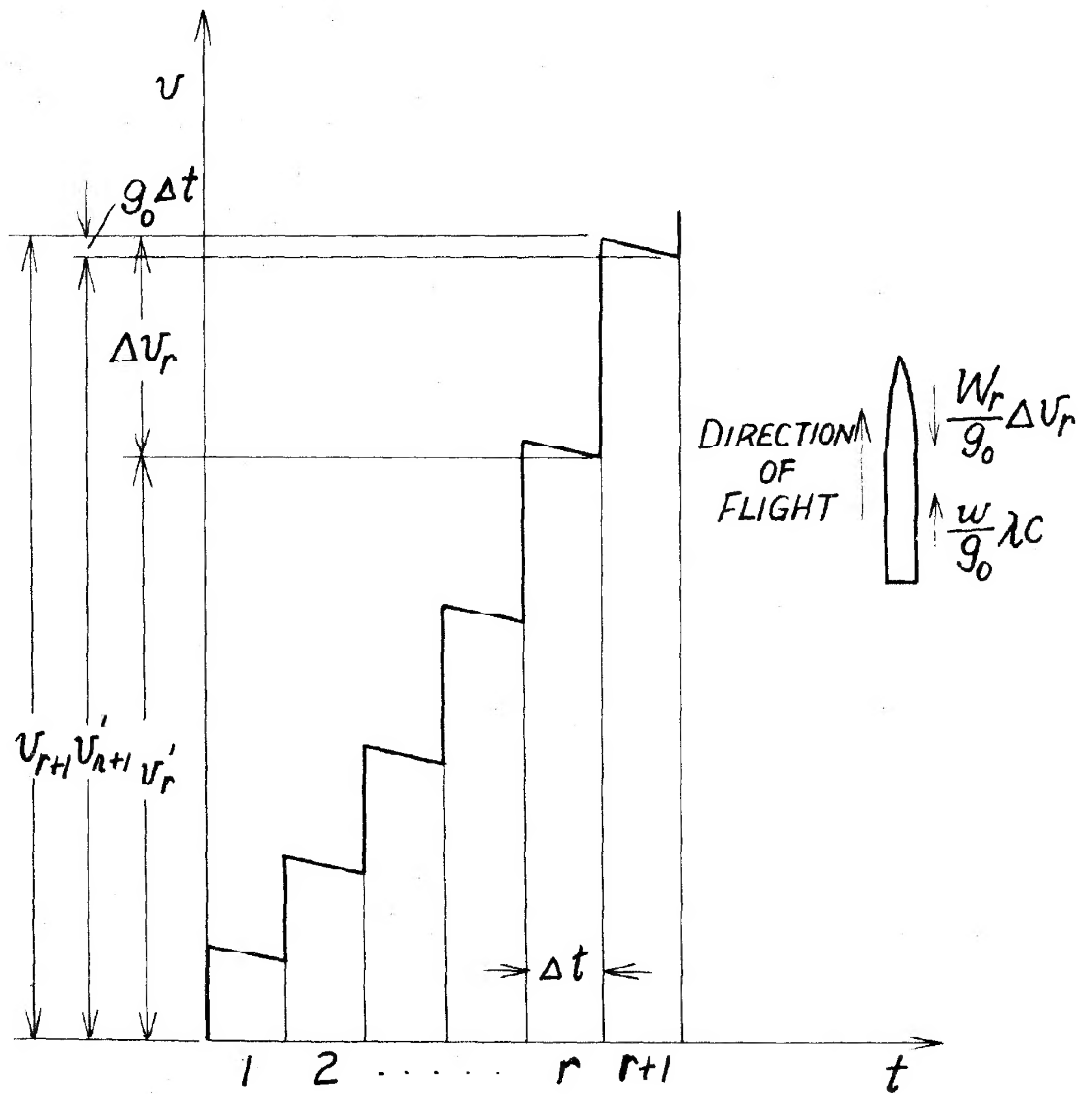


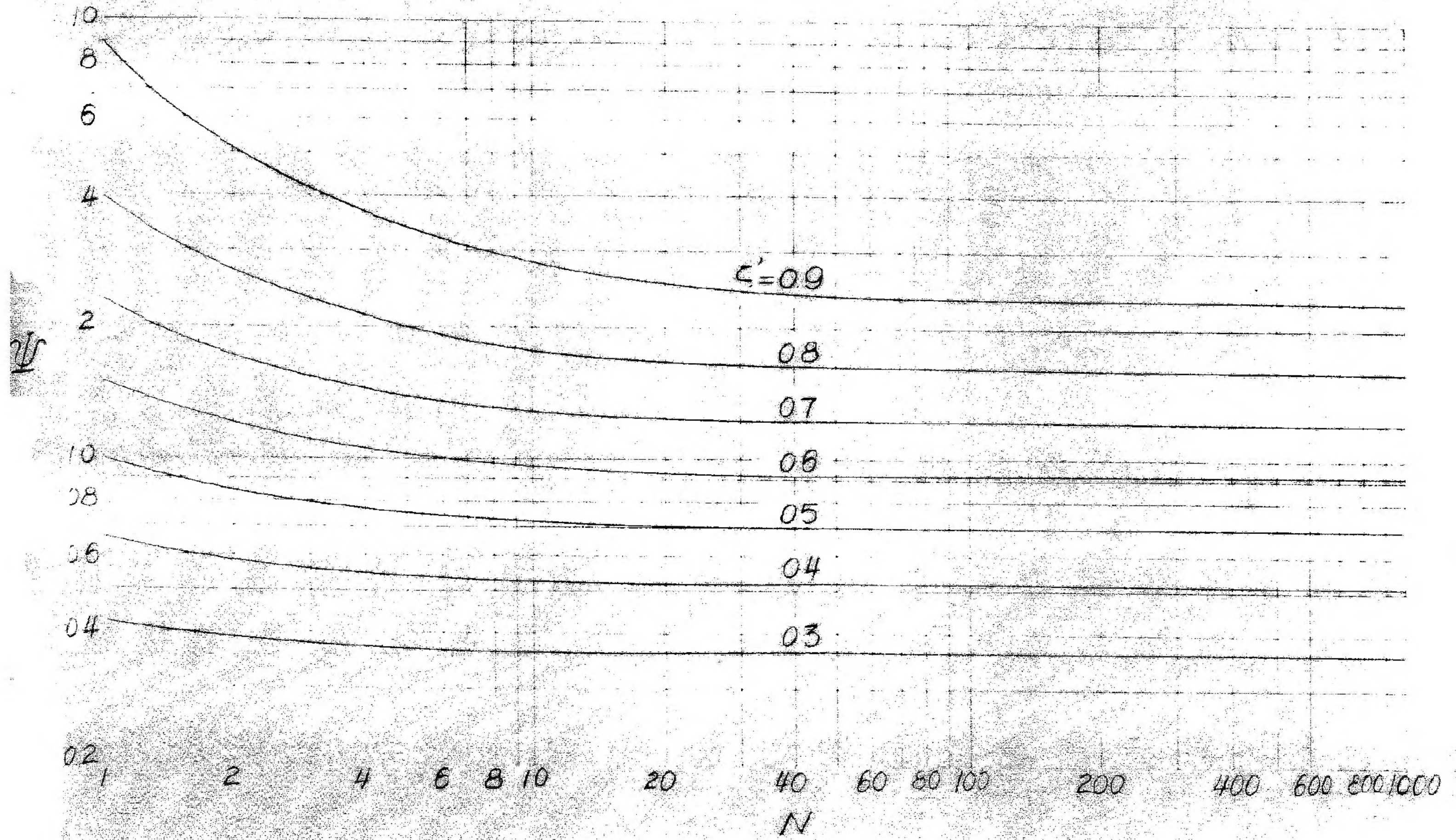
Fig. 3.5 Effect of compressibility on the pressure distribution of Joukowsky airfoil with b=0.20



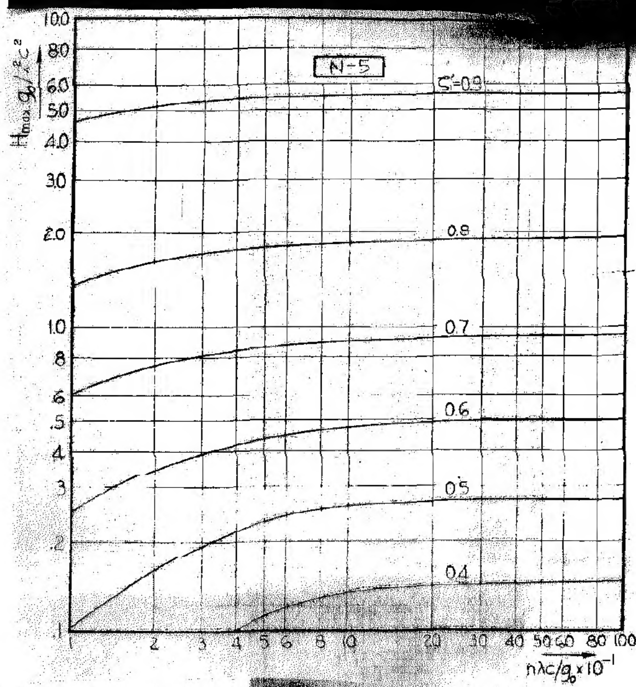
v
$g_o \Delta t$
Δv_r
v_{r+1} v'_{r+1} v'_r
DIRECTION OF FLIGHT
$\frac{W_r}{g_o}\Delta v_r$
$\frac{w}{g_o}\lambda c$
Δt
1 2 . . . . . . r r+1
t

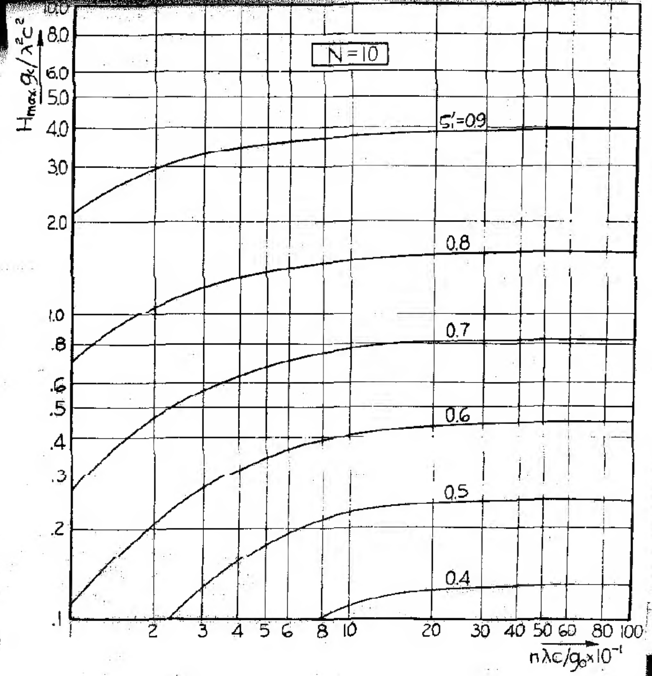
Fig. 4.1

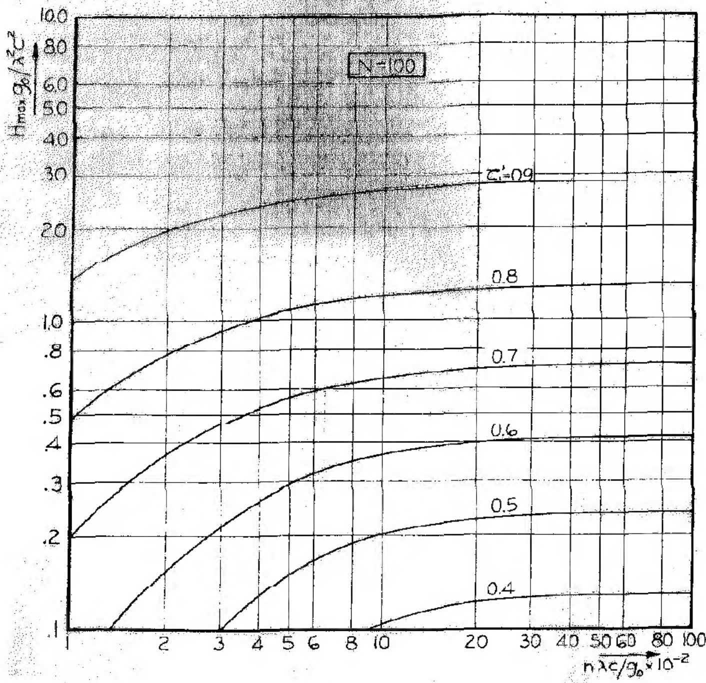
Fig. 4.2



10
8
6
4
2
Ψ
10
08
06
04
02
ς'=09
08
07
06
05
04
03
1
2
4
6
8
10
20
40
60
80
100
200
400
600
800
1000
N







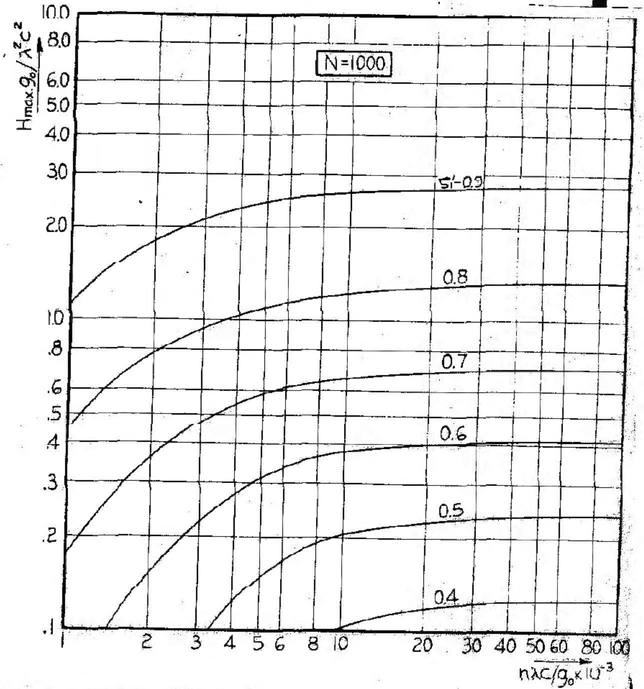


Fig. 4.3

$$\frac{H_{max}\,g_0}{\lambda^2 c^2} = \frac{1}{2}\Psi^2 - \frac{1}{\frac{n\lambda c}{g_0}}\left[\left(\frac{N}{\varsigma_1'} - 1\right)\Psi - N\right]$$